New Fe-Cu bimetallic coordination compounds based on ω-ferrocene carboxylic acids and 2-thioimidasol-4-ones: structural, mechanistic and biological studies

Guk D.A., Krasnovskaya O.O., Moiseeva A.A., Tafeenko V.A., Ul'yanovskii N.V., Kosyakov D.S., Pergushov V.I., Melnikov M.Ya., Zyk N.V., Skvortsov D.A., Lopatukhina E. V., Vaneev A.N., Gorelkin P.V., Erofeev A.S., Majouga A.G., Beloglazkina E.K.

Supplementary information

1. Electrochemical measurements

Elecrtochemical experiments were carried out using a IPC ProM potentiostat by cyclic voltammetry (CV) and rotating disk electrode (RDE) techniques. Glass-carbon (d=2mm) disks were used as the working electrodes, 0.05M Bu_4NClO_4 solution in CH_3CN served as the supporting electrolyte, and Ag/AgCl/KCl(satur.) was used as the reference electrode. The numbers of electrons transferred in each steps of the redox processes were determined in RDE experiments comparing the magnitude of the wave current with the current of single-electron oxidation of ferrocene, taken in equal concentration. The potential scan rates were $100mVs^{-1}$.

All measurements were carried out under argon. The samples were dissolved in the pre-deaerated solvent. Acetonitrile (high purity grade) was additionally purified by reflux with phosphorus pentaoxide followed by distillation.

2. Single crystall X-ray diffraction analysis

The data of **14a** were collected at room temperature by using STOE diffractometer Pilatus100K detector, focusing mirror collimation Cu Kα (1.54086Å) radiation, rotation method mode. STOE X-AREA software was used for cells refinement and data reduction. Data collection and image processing was performed with X-Area 1.67 (STOE &Cie GmbH, Darmstadt, Germany, 2013). Intensity data were scaled with LANA (part of X-Area) in order to minimize differences of intensities of symmetry-equivalent reflections (multi-scan method)."

The data of **12a** were collected at 120K by using Bruker APEX2 DUO diffractometer (MoKα, radiation graphite monochromator, ω -scan mode).

The structures were solved with SHELXT and refined with SHELX (**14a**) and Olex22 (**12a**) programs. The crystals of (**14a**) are very small and twinned, which is reflected in the results obtained. For example, the accuracy of bond lengths is not higher than 0.01-0.02 angstroms.

The non-hydrogen atoms (for both substances) were refined by using the anisotropic full matrix least-square procedure. All hydrogen atoms were placed in the calculated positions and allowed to ride on their parent atoms [C-H 0.93-0.98; Uiso 1.2 Ueq (parent atom)].

CCDC-2079489 (**14a**) and 2079490 (**12a**) contain the supplementary crystallographic data for this paper. These data can be obtained free of charge from The Cambridge CrystallographicData Centre via www.ccdc.cam.ac.uk/data_request/cif.

The structure of copper(I) perchlorate released as a product of the interaction of ligands 11a-e with copper (II) perchlorate was also confirmed by X-ray diffraction analysis (Fig. S1).
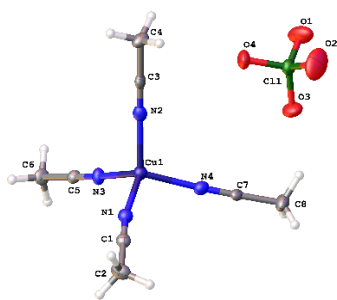
Fig. S1. Cu(CH$_3$CN)$_4$ClO$_4$ molecular structure.

Table S1. Basic crystallographic data and refinement parameters for Cu(CH$_3$CN)$_4$ClO$_4$.

	Cu(CH$_3$CN)$_4$ClO$_4$
Chemical formula	C$_8$H$_{12}$ClCuN$_4$O$_4$
Molecular weight	327.21
T, K	120
Crystal system	Ромбическая
Space group	P2$_1$2$_1$2$_1$
Z	12
Z'	3
a, Å	8.3427(11)
b, Å	20.394(2)
c, Å	23.826(3)
α, °	90
b, °	90
γ, °	90
V, Å^3	4053.9(8)
D$_{calc}$, g×cm^{-3}	1.608
m, cm^{-1}	18.25
F(000)	1992
2q$_{max}$, °	60
Number of recorded reflections	29348
Numberofindependentreflections	12410
Number of reflections with I>2s(I)	7699
Number of parameters to be specified	500
R1	0.0578
wR2	0.1202
GOF	0.960
Residual electron density, e×Å^{-3} (d$_{max}$/d$_{min}$)	0.768/-0.638

3. UV-vis Spectroscopy
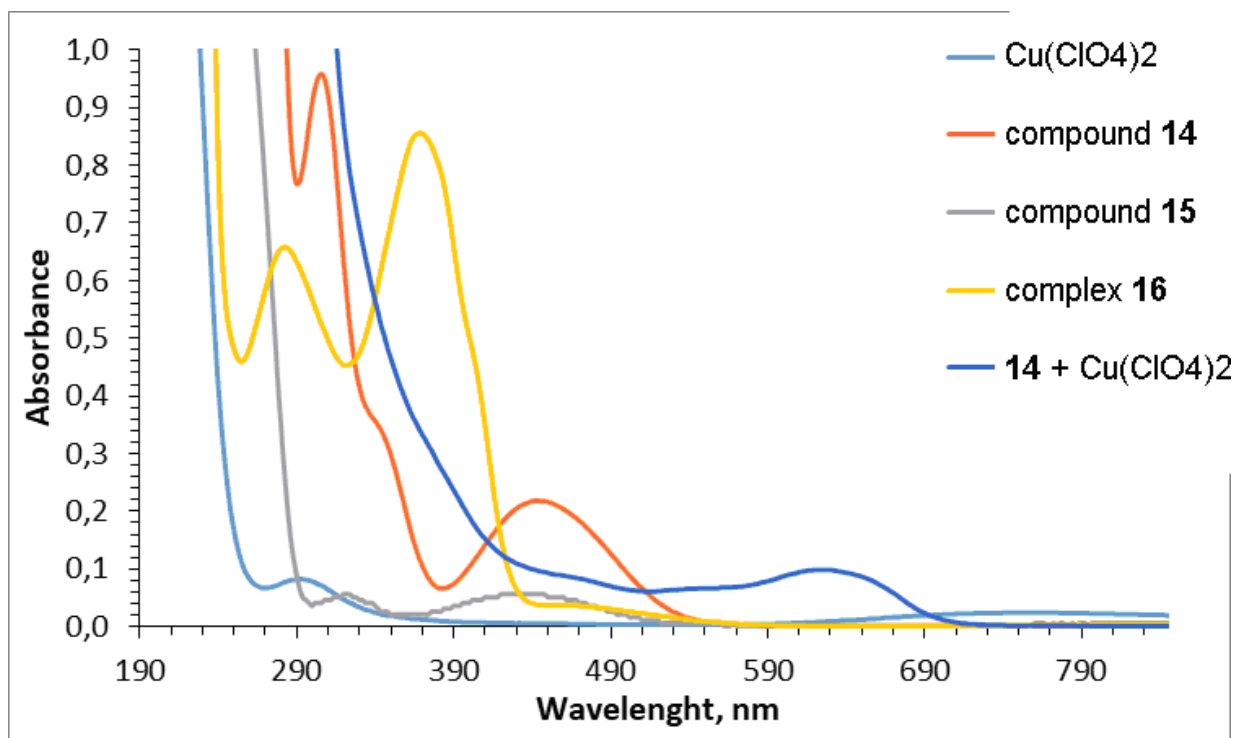
Fig. S2. UV-vis absorption spectra of model ferrocenes **14**, **15**, copper(+2) 2-thioimidazolone complex **16**, $Cu(ClO_4)_2 \cdot 6H_2O$ and products of their interactions in acetonitrile, C = 10^{-4}M.
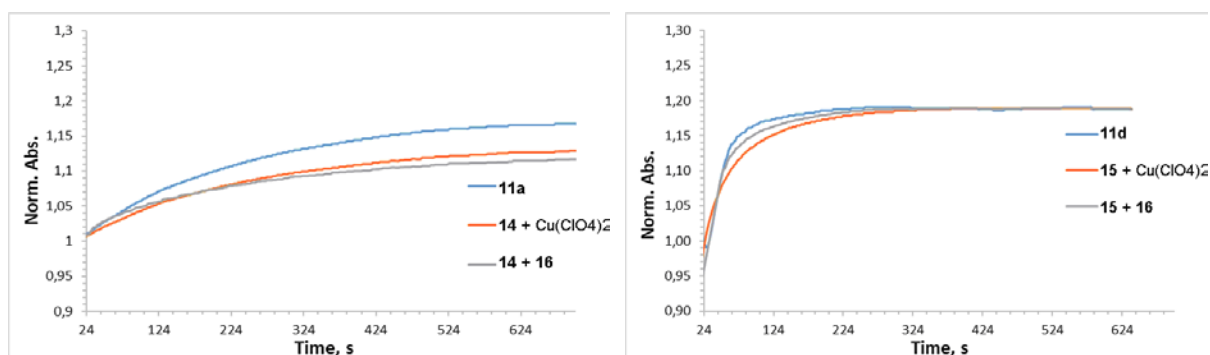
Fig. S3. Kinetic curves of Fc^+ accumulation, recorded by the change in the optical density on 437 nm wavelength for the mixtures of model ferrocenes **14, 15** with $Cu(ClO_4)_2 \cdot 6H_2O$ or complex **16** in CH_3CN. Starting concentrations of both reagents was 10^{-4}M.

4. EPR Spectroscopy

EPR spectra were recorded on a Varian E-3 EPR spectrometer at the boiling point of liquid nitrogen (77.4K). Equimolar solutions of copper(II) perchlorate hexahydrate and organic ligand **13a** or **13d** were mixed just before the measurement. Samples of reaction mixture were sealed in a capillary and frozen to the boiling point of liquid nitrogen. By the change of the integral intensity of the signal of paramagnetic nuclei, a kinetic curve was plotted and processed by methods of mathematical analysis to study the reaction mechanism.

During the study, it was found that the measured concentration of Cu^{2+} ions when dissolving a sample of copper perchlorate (II) in pure acetonitrile changes over time (Fig. S2). For further experiments with ligands **13a** or **13d**, a solution of copper perchlorate in acetonitrile was kept for 15 minutes to achieve a constant Cu^{2+} signal.
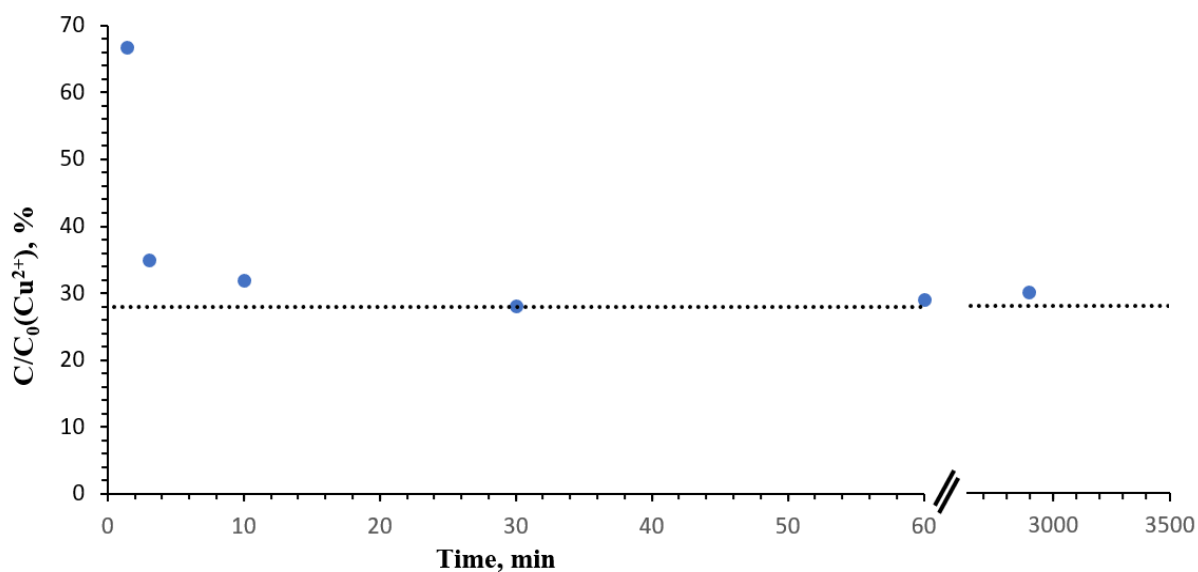
Fig. S4. Change in the detected concentration of Cu^{2+} with time when the sample of $Cu(ClO_4)_2*6H_2O$ is dissolved in acetonitrile.

6. Real-time HRMS monitoring

The reaction was carried out at a concentration of each component of 10^{-4} M. Weighed portions of the starting reagents were dissolved in HPLC grade acetonitrile and mixed in the required ratio. After that, the solution was immediately withdrawn into a 1 ml glass syringe, connected by a capillary to the ion source of the mass spectrometer, and the syringe was placed in a KDS syringe pump.

The following program was used to supply the solution to the source: 10 seconds - 300 µL/min, then 10 µL/min for 50 minutes.

Mass spectrometer parameters: ESI (+), gas flows (psi) CUR = 25.000, GS1 = 15.000, GS2 = 0.000, without heating, needle voltage 5500 V, declusterization potential 20 V. The spectrum was recorded in the m / z range 100- 1200, accumulation time 250 ms. Recording was started immediately after setting the flow rate from the syringe pump to 10 µL/min.

The total ionic current (TIC) chromatogram of the reaction mixture is shown in Figure S5.
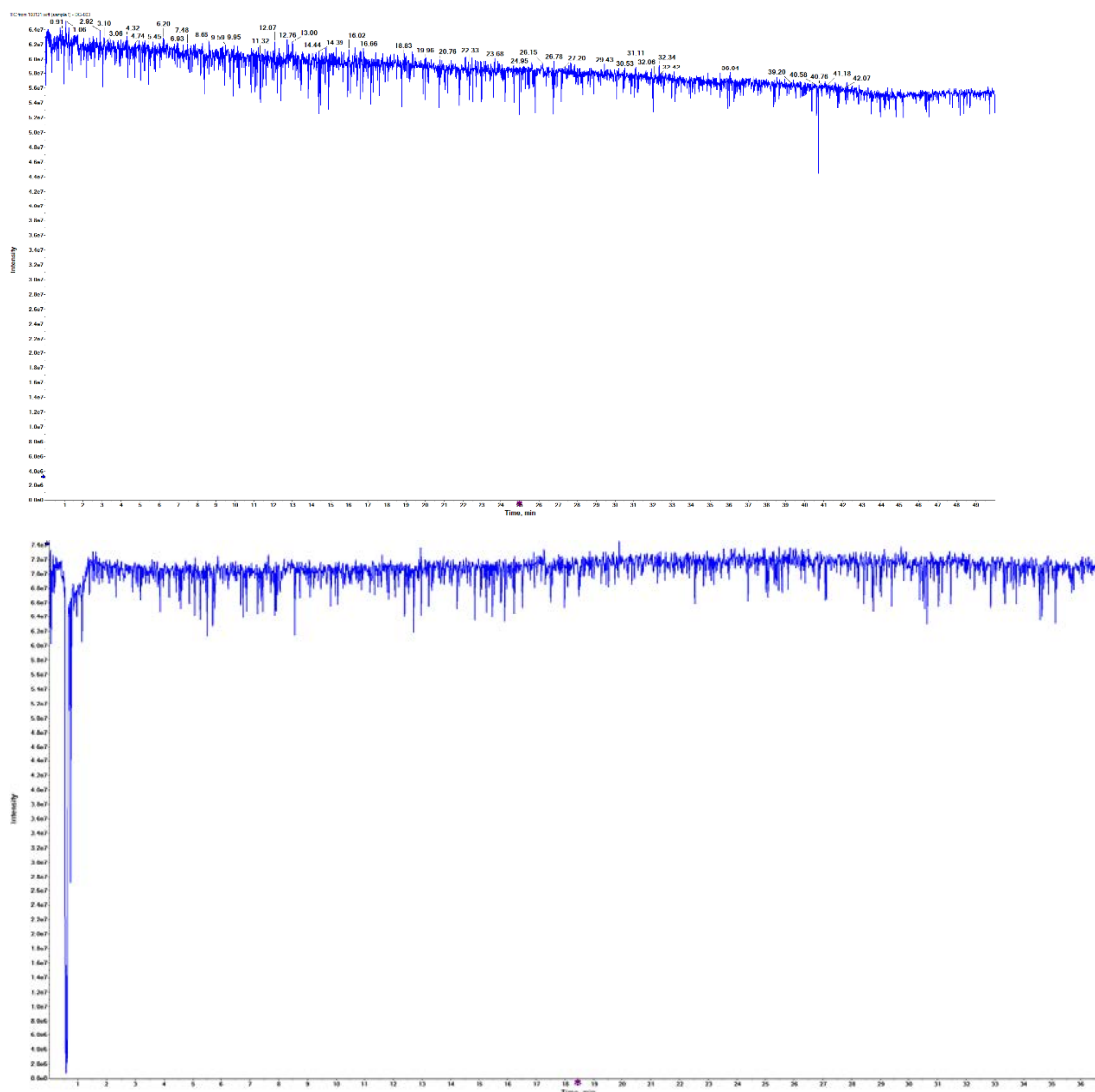
Fig. S5. Time dependence of the mass spectrometric signalfor mixtures of 11a (above) and 11d (below) with $Cu(ClO_4)_2 \cdot 6H_2O$.

5.1 Real time HRMS monitoring for reaction of 11a with $Cu(ClO_4)_2·6H_2O$.

Mass spectra at the beginning of the reaction and at the end are shown in Figure S6.
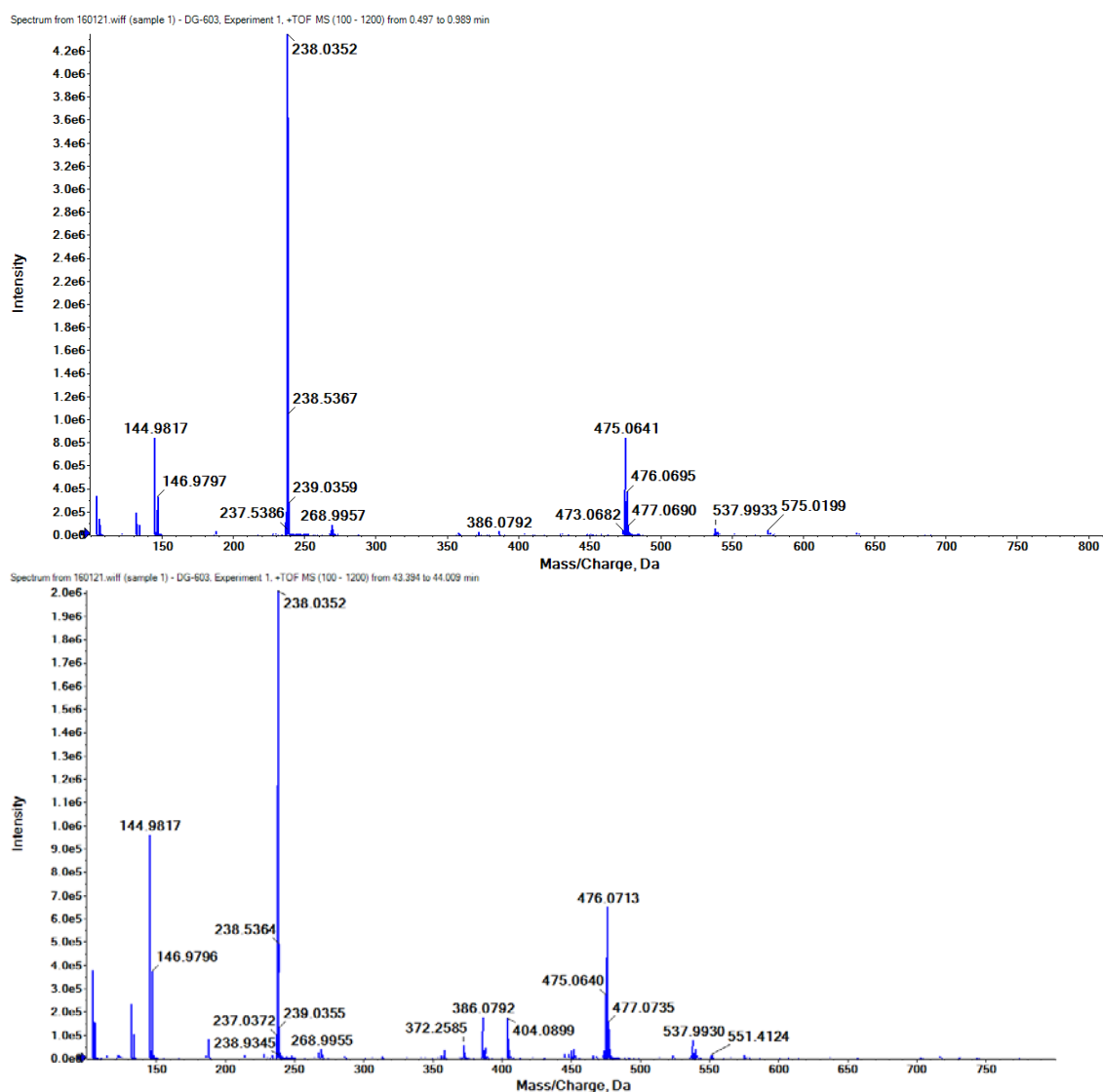
Fig. S6. Mass spectra of the reaction mixture of 11a with $Cu(ClO_4)_2*6H_2O$ at the beginning (top) of the reaction and after the end of the interaction (bottom)..

Presumptive identification of the components present in the reaction mixture:

m/z 103.9558 Elemental composition $[C_2H_3NCu^{2+}]^+$ = Copper-Acetonitrile adduct.

m/z 144.9817 Elemental composition $[C_4H_6N_2Cu^{2+}]^+$= Copper-2xAcetonitrile adduct.
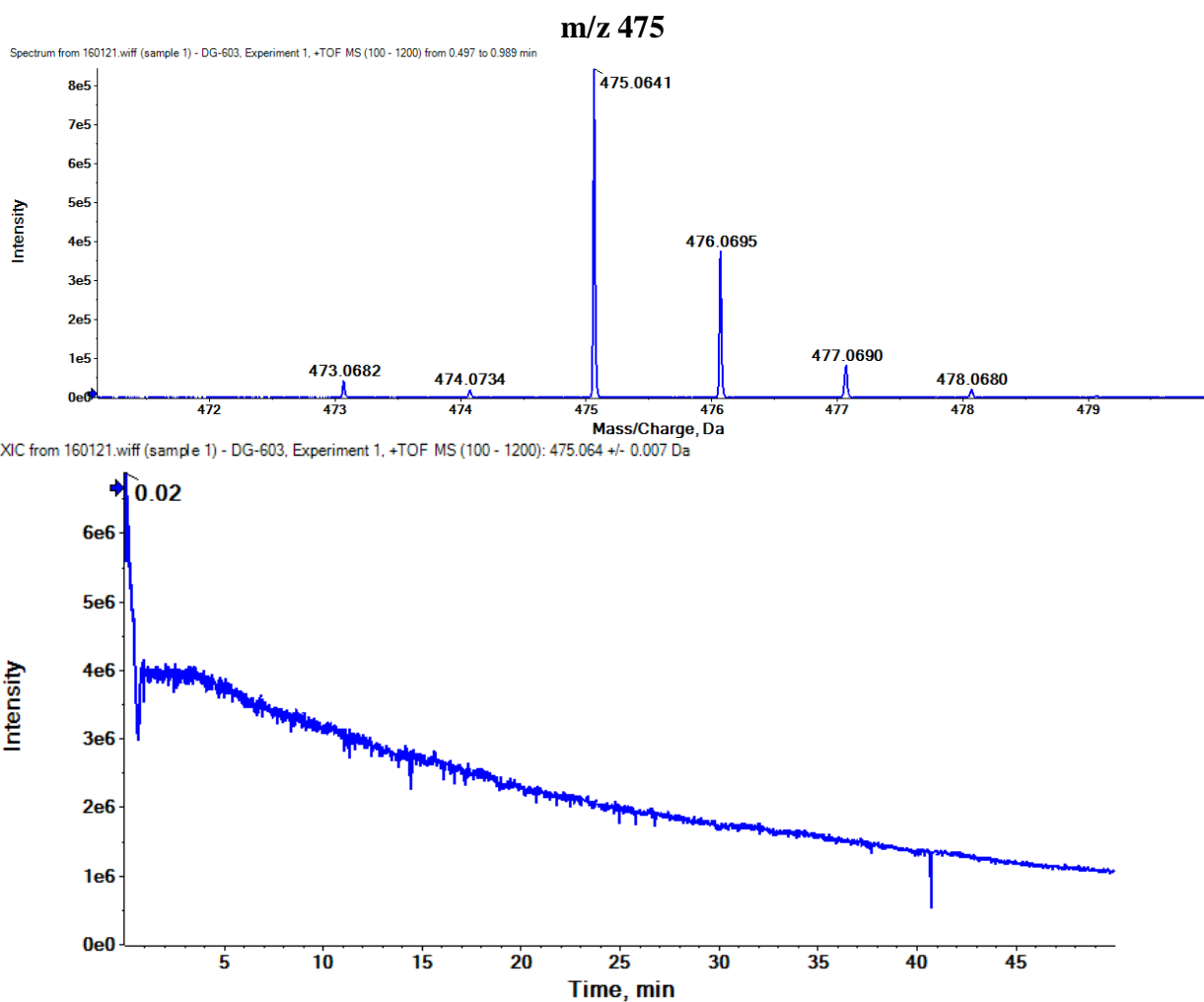
Fig. S7. Ion with m/z 475 in spectra (above) and ion current for described ion (below).

Elemental composition $[C_{23}H_{21}FeN_3O_3S]^+$.

This ion is not a protonated molecule, the ion is formed due to the presence in the structure of Fe^{3+} = $[\textbf{11a}\text{-}Fe^{3+}]^+$.

The intensity of this ion decreases with time, at the end of the interaction the already protonated molecule $[M+H]^+$ (m/z = 476) predominates, which is clearly seen in Figure S75.

m/z 538

Spectrum from 160121.wiff (sample 1) - DG-603, Experiment 1, +TOF MS (100 - 1200) from 0.497 to 0.989 min

XIC from 160121.wiff (sample 1) - DG-603, Experiment 1, +TOF MS (100 - 1200): 537.993 +/- 0.010 Da
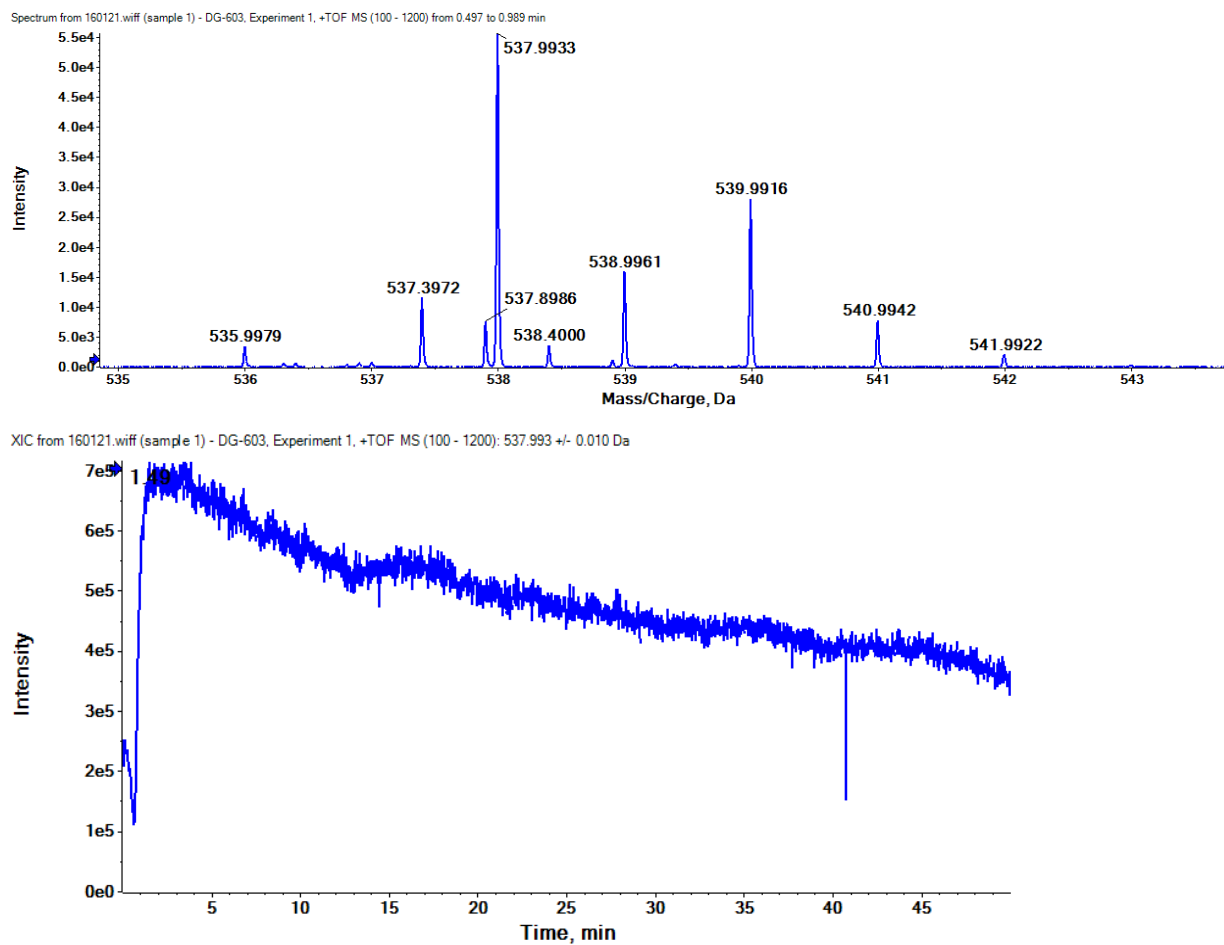
Fig. S8. Ion with m/z 538 in spectra (above) and ion current for described ion (below).

Elemental composition $[C_{23}H_{21}FeCuN_3O_3S]^+$. Delta -2.0 ppm

Ion is formed by the coordination of copper – $[\mathbf{11a}\text{-}Fe^{2+}+Cu^+]^+$

This ion is formed in the first minutes of the reaction, after which its intensity in the spectrum gradually decreases. The spectrum of this component also contains an impurity ion with a charge of 2 (m/z = 537.3972).

m/z 637
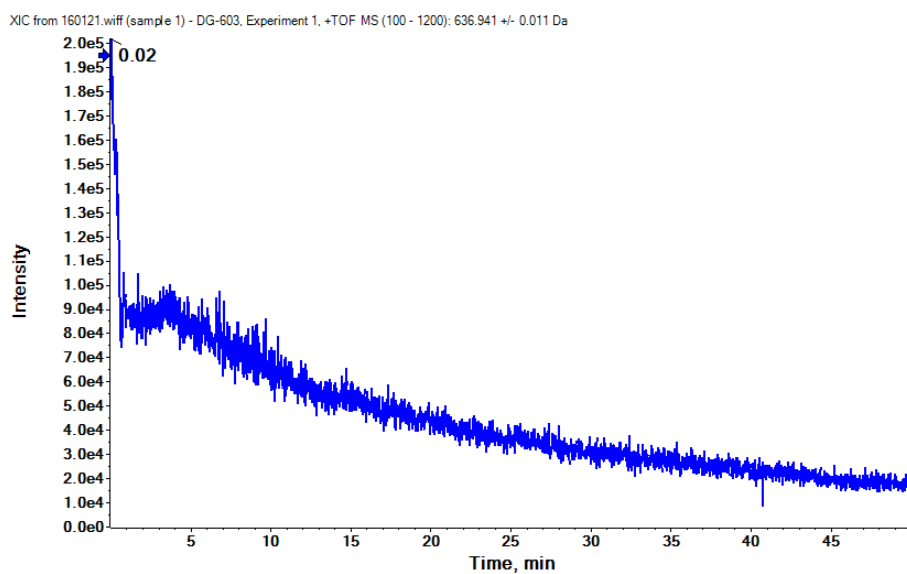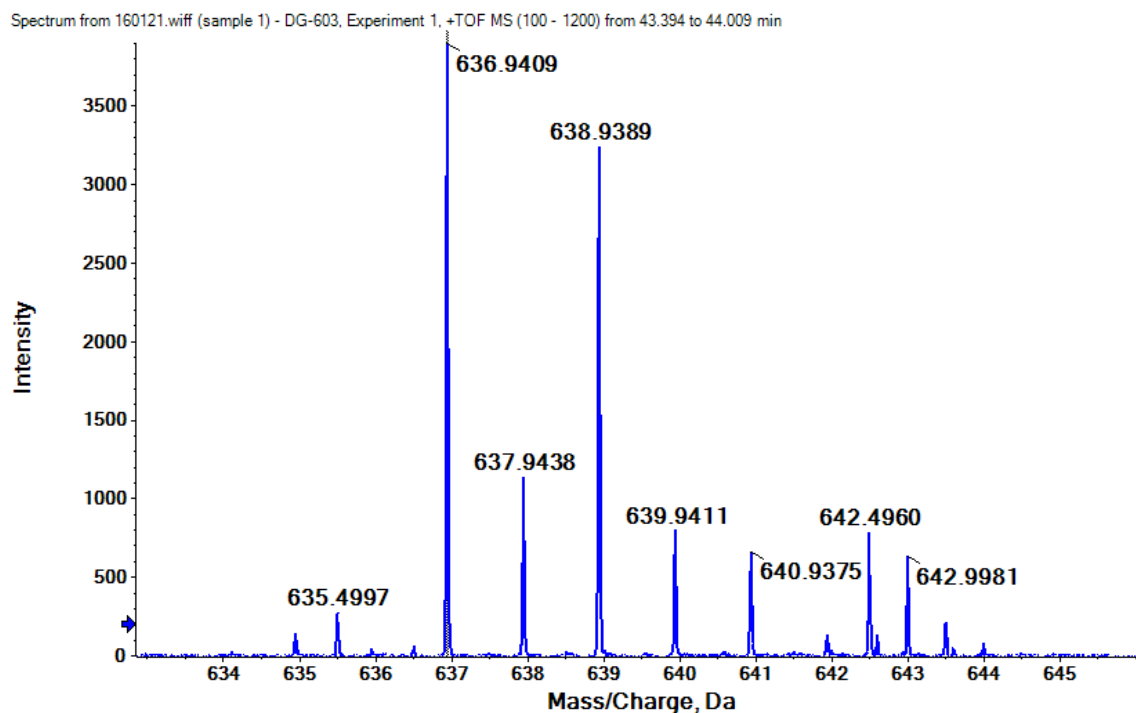
Fig. S9. Ion with m/z 637 in spectra (above) and ion current for described ion (below).

Elemental composition $[C_{23}H_{21}FeCuN_3O_7SCl]^+$. Delta -3.0 ppm

By analogy with **11d**, it can be assumed that the ion is formed by the addition of $[ClO_4]^- = [[\textbf{11a}\text{-}Fe^{3+}+Cu^+]^{2+}[ClO_4]^-]^+$.

m/z 269

Spectrum from 160121.wiff (sample 1) - DG-603, Experiment 1, +TOF MS (100 - 1200) from 0.456 to 0.948 min
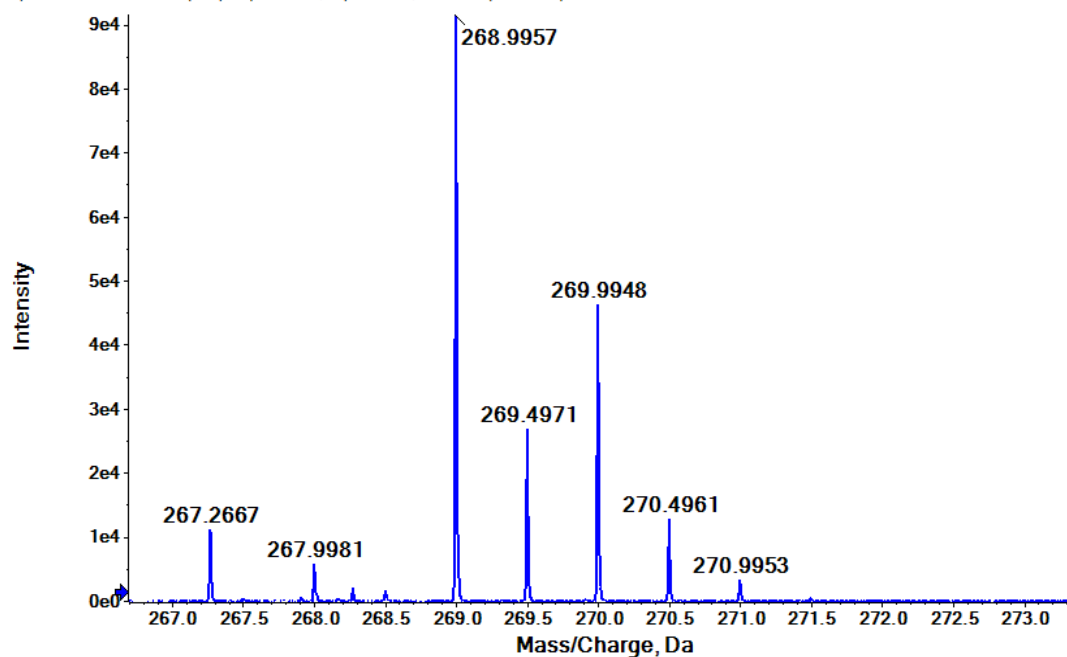
XIC from 160121.wiff (sample 1) - DG-603, Experiment 1, +TOF MS (100 - 1200): 268.995 +/- 0.005 Da
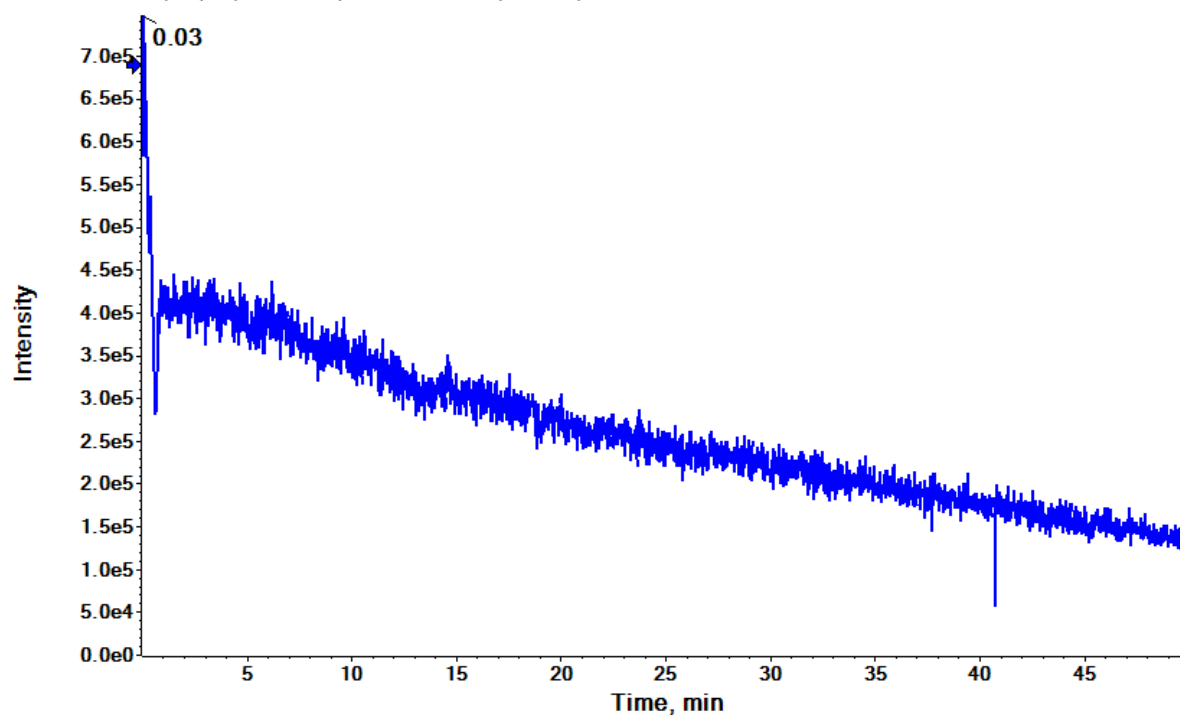
Fig. S10. Ion with m/z 269 in spectra (above) and ion current for described ion (below).

Double-charged ion, Elemental composition $[C_{23}H_{21}FeCuN_3O_3S]^{2+}$, Delta -4.5 ppm.

Ion can be formed in two ways: $[\mathbf{11a}\text{-}Fe^{3+}+Cu^+]^{2+}$ or $[\mathbf{11a}\text{-}Fe^{2+}+Cu^{2+}]^{2+}$. The intensity in the spectrum also decreases with time.

m/z 238

Spectrum from 160121.wiff (sample 1) - DG-603, Experiment 1, +TOF MS (100 - 1200) from 0.456 to 0.948 min
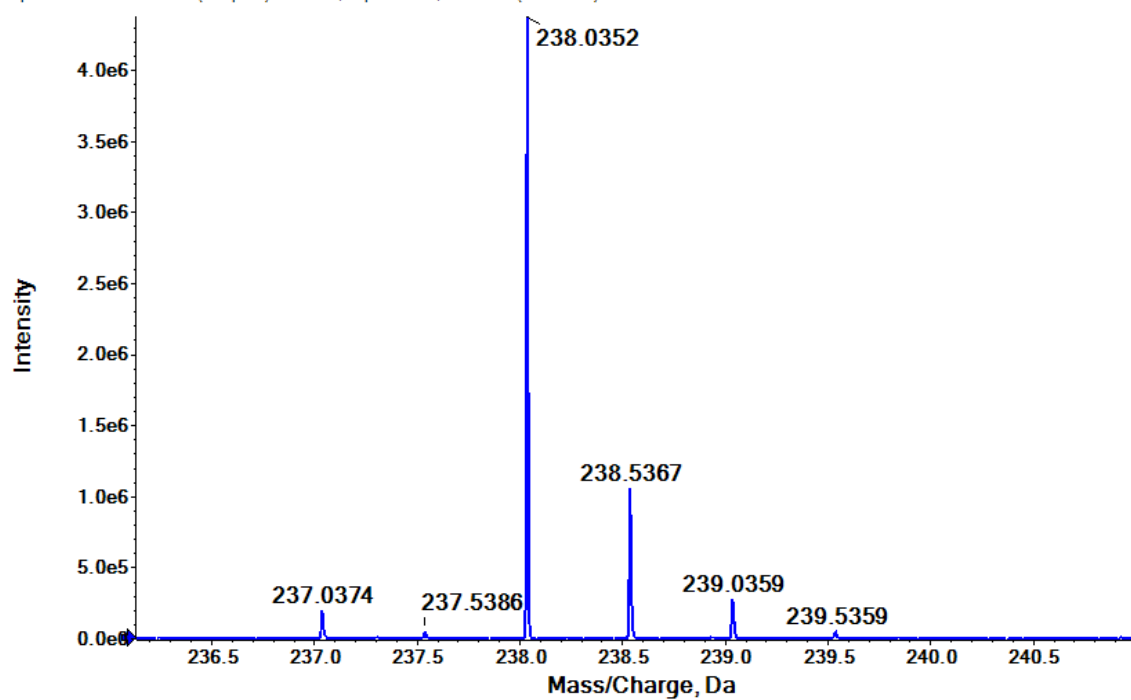
XIC from 160121.wiff (sample 1) - DG-603, Experiment 1, +TOF MS (100 - 1200): 238.0351 +/- 0.0036 Da
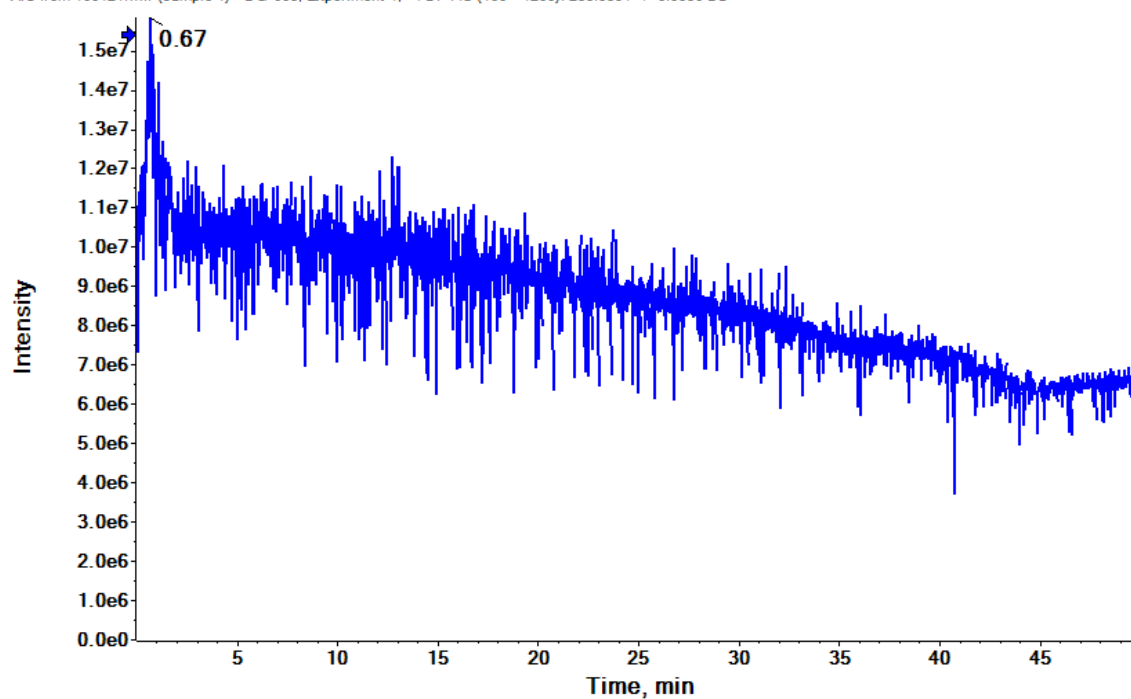
Fig. S11. Ion with m/z 238 in spectra (above) and ion current for described ion (below). Double-charged ion, Elemental composition $[C_{23}H_{22}FeN_3O_3S]^{2+}$, Delta -3.6 ppm. Molecule protonated, ion formed = $[\mathbf{11a}\text{-}Fe^{3+}+H^+]^{2+}$
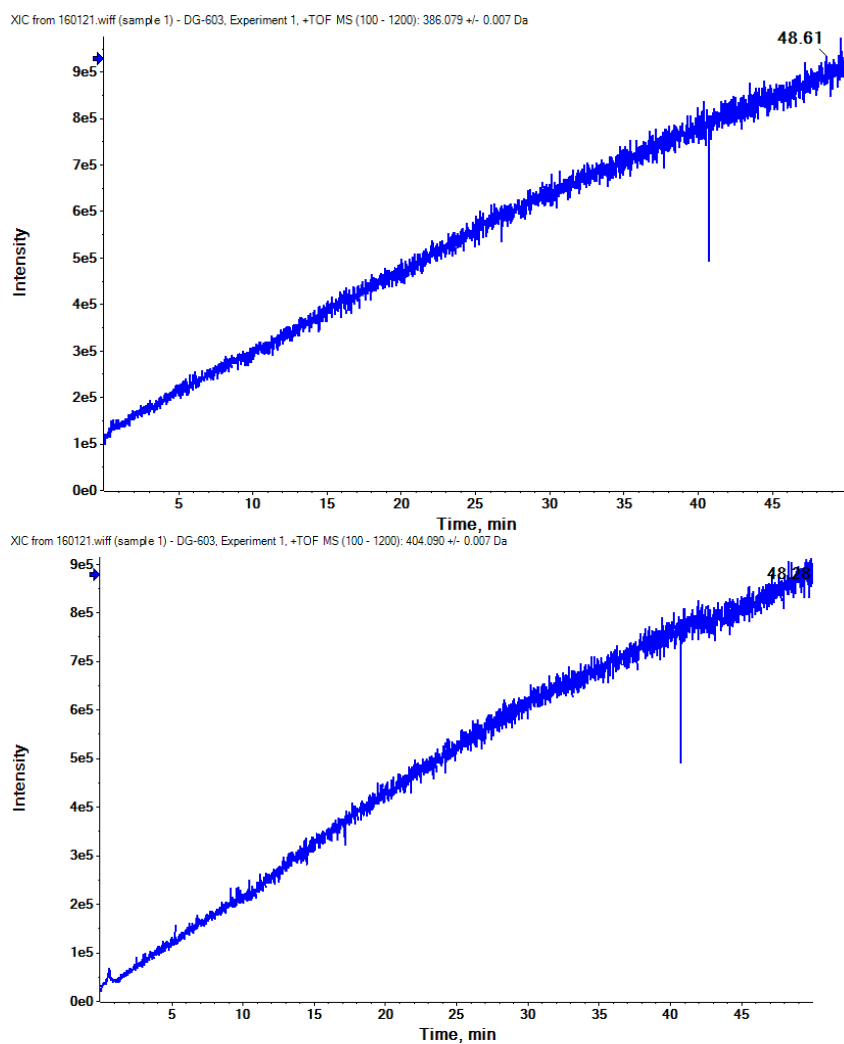
Fig. S12. Ion current for ions m/z 386 (above) and 404 (below).

5.2 Real time HRMS monitoring for reaction of 11d with $Cu(ClO_4)_2*6H_2O$.

It should be noted that within 40 minutes from the start of the reaction, the mass spectrum of the reaction mixture and the ratio of individual ions to the spectrum remains constant, with the exception of the first ~ 2 min. Examples of mass spectra are shown in Figure S13.
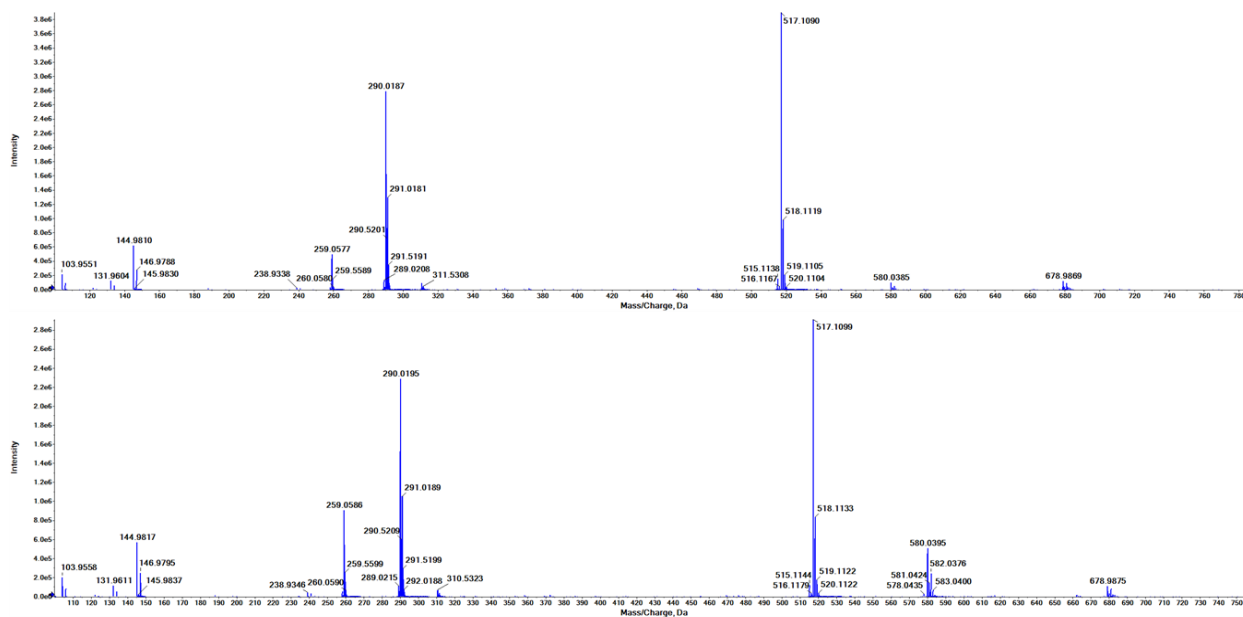
Fig. S13. Mass spectra of the reaction mixture of 11d with $Cu(ClO_4)_2*6H_2O$ at the beginning (top) of the reaction (~ 1 min after mixing the reagents) and after the end of the interaction (bottom).

The spectra are characterized by a similar set of ions, however, at the beginning of the reaction, ions with m/z 259 and 580 have a lower intensity. After ~ 2 minutes from the beginning of the reaction, their intensities in the spectra increase and remain constant throughout the studied period of time (40 minutes). Examples of mass-extracted chromatograms are shown in Figure S13.
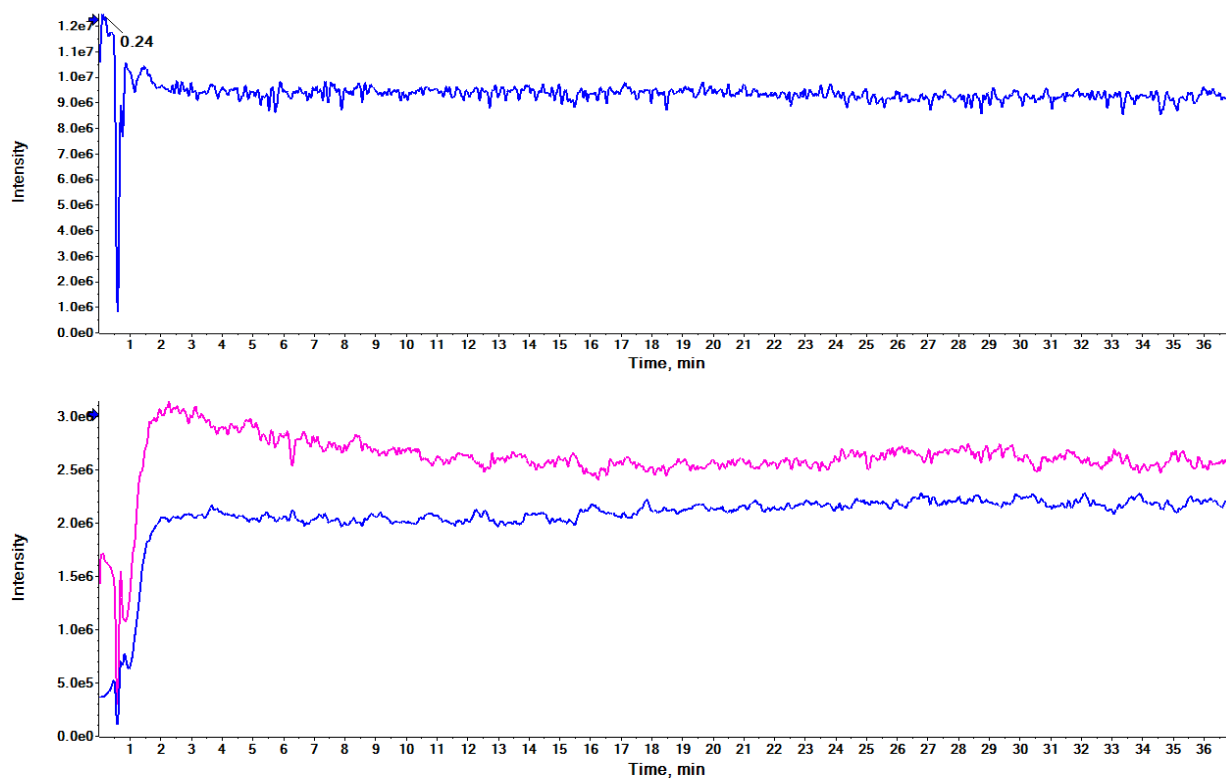
Fig. S14. Time dependence of the mass spectrometric signalfor exact masses for components with m/z 517 (top), 259 - pinc and 580 - blue (bottom).

The chromatograms shown in Fig. S13, S14 confirm that the detected components are formed at the initial time. No further visible changes were observed.

m/z 103.9558 Elemental composition $[C_2H_3NCu^{2+}]^+$ = Copper-Acetonitrile adduct,as incase of **11a**.

m/z 144.9817 Elemental composition $[C_4H_6N_2Cu^{2+}]^+$ = Copper-2·Acetonitrile adduct, as in case of **11a**.

m/z 517
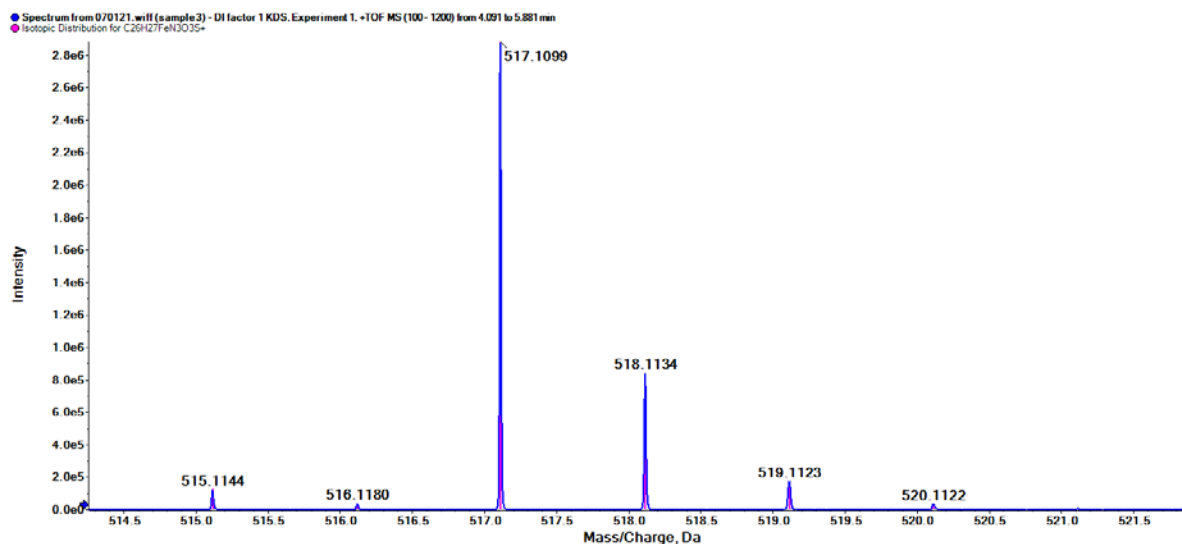
Fig. S15. Ion with m/z 517 in spectra (above) and ion current for described ion (below).

Elemental composition $[C_{26}H_{27}FeN_3O_3S]^+$, Delta -3.5 ppm.

This ion is not a protonated molecule, the ion is formed due to the presence in the structure of $Fe^{3+} = [\textbf{11d}\text{-}Fe^{3+}]^+$.

m/z 580
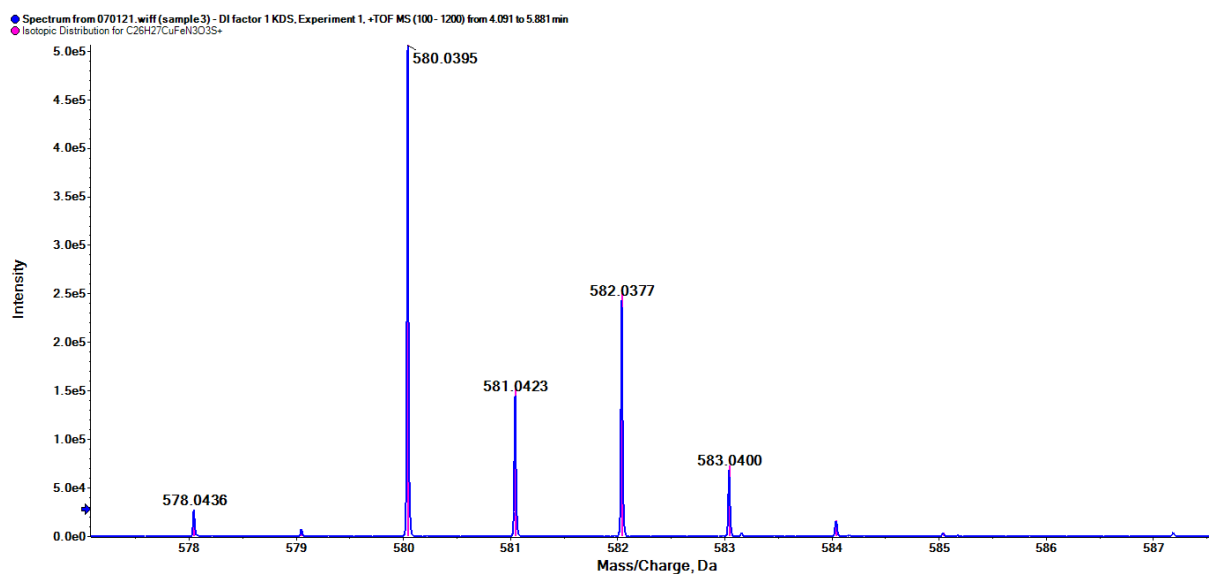
Fig. S15. Ion with m/z 580 in spectra.

Elemental composition $[C_{26}H_{27}FeN_3O_3SCu]^+$, Delta -3.1 ppm.

Ion is formed by the coordination of copper – $[\textbf{11d}\text{-}Fe^{2+}+Cu^+]^+$

m/z 662
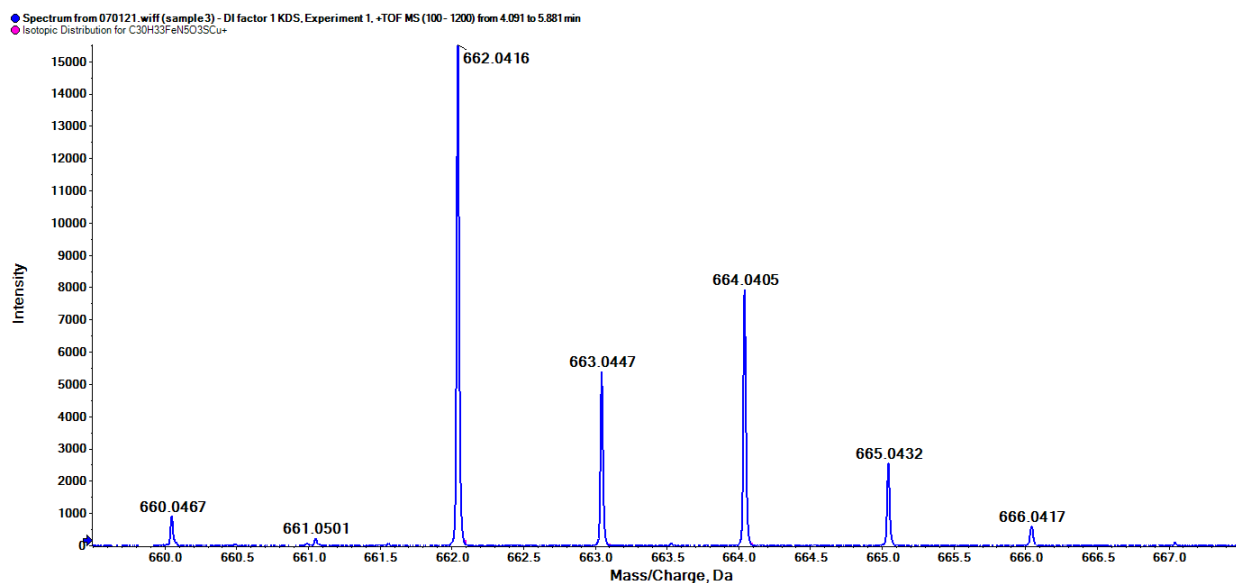
Fig. S17. Ion with m/z 662 in spectra.

Elemental composition $[C_{30}H_{33}FeN_5O_3SCu]^+$

Based on fragmentation and isotopic structure, the following structure is proposed: $[\mathbf{11d}\text{-}Fe^{2+}+Cu^++(CH_3CN)_2]^+$

m/z 678
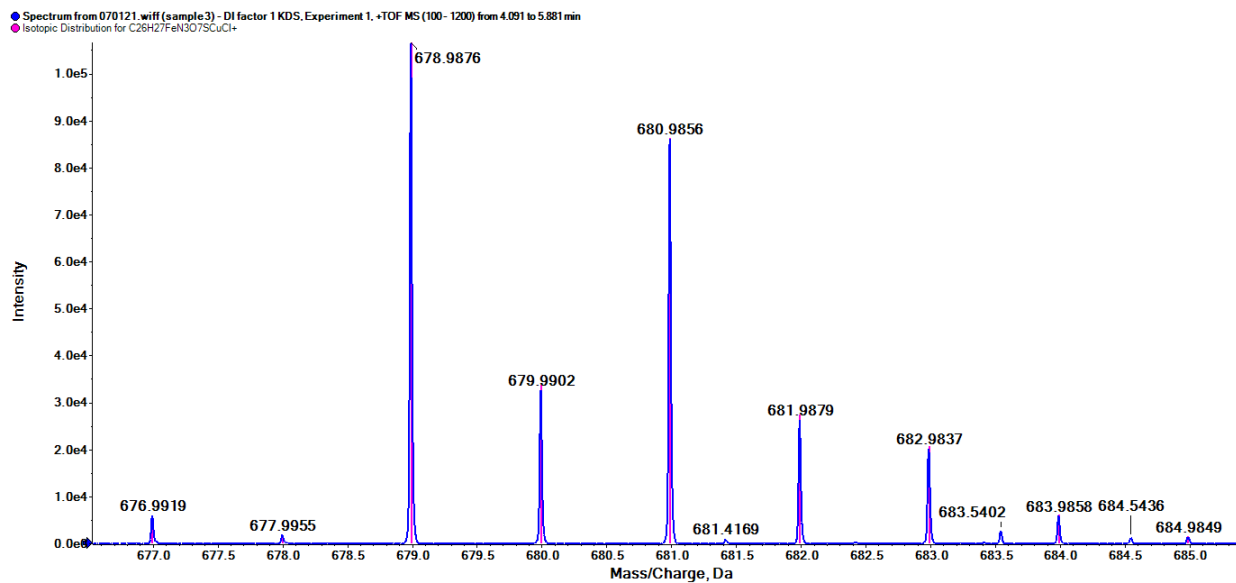
Fig. S18. Ion with m/z 678 in spectra.

Elemental composition $[C_{26}H_{27}FeN_3O_7SCuCl]^+$, Delta -3.3 ppm,

Based on fragmentation and isotopic structure, the following structure is proposed: = $[[\mathbf{11d}\text{-}Fe^{3+}+Cu^+]^{2+}[ClO_4]]^+$

m/z 310
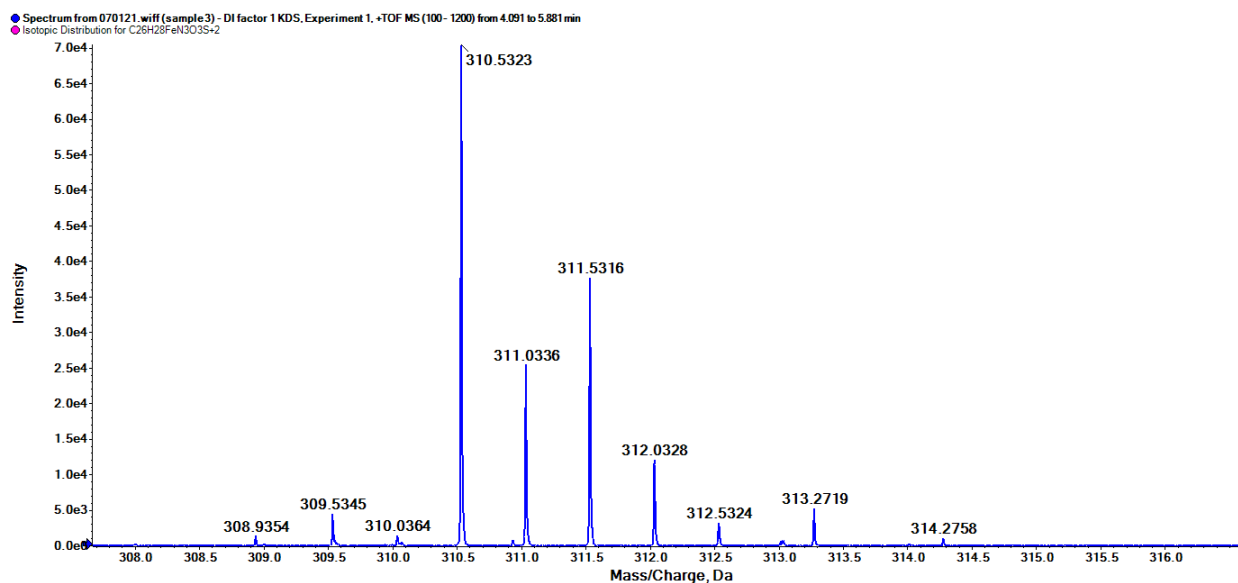
Fig. S19. Ion with m/z 310 in spectra.

Double-charged ion, Elemental composition $[C_{28}H_{30}FeCuN_4O_3S]^{2+}$

Possible ion structures are $[\textbf{11d}\text{-}Fe^{2+}+Cu^{2+}+AcN]^{2+}$ or $[\textbf{11d}\text{-}Fe^{3+}+Cu^++AcN]^{2+}$

m/z 290
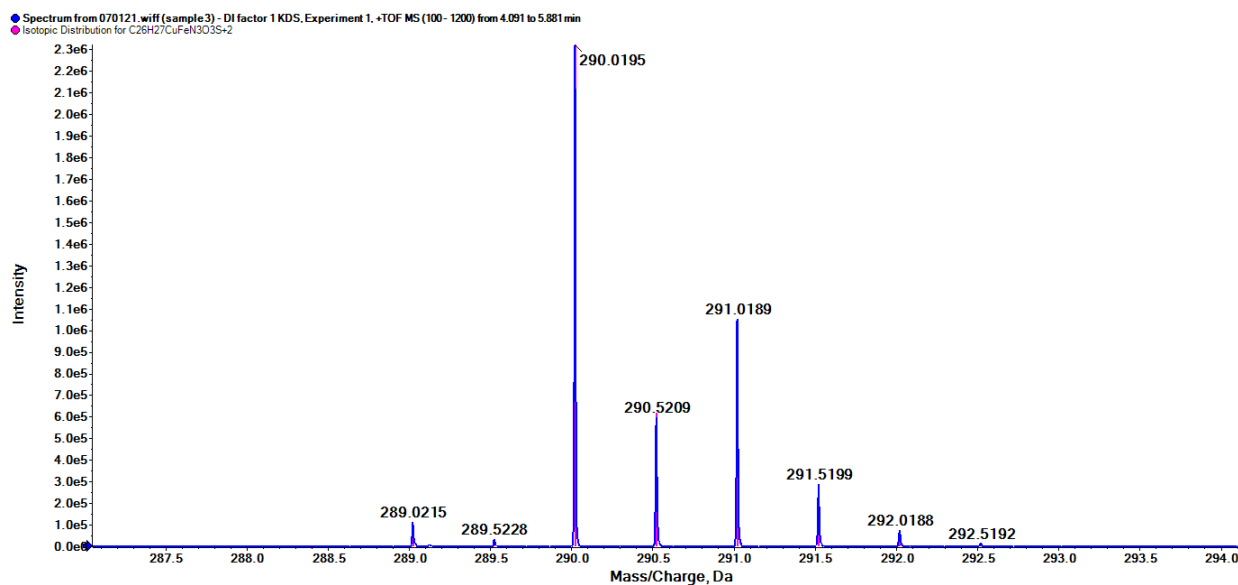
Fig. S20. Ion with m/z 290 in spectra.

Double-charged ion, Elemental composition $[C_{26}H_{27}FeN_3O_3SCu]^{2+}$, Delta -3.1 ppm

Possible ion structures are $[\textbf{11d}\text{-}Fe^{3+}+Cu^+]^{2+}$ or $[\textbf{11d}\text{-}Fe^{2+}+Cu^{2+}]^{2+}$, however, MS-MS experiments show that the structure $[\textbf{11d}\text{-}Fe^{3+}+Cu^+]^{2+}$ is most plausible, due to the fact, that peaks of fragment ions always contain a methylene-ferrocenium ion of the cation with a high intensity.

m/z 199
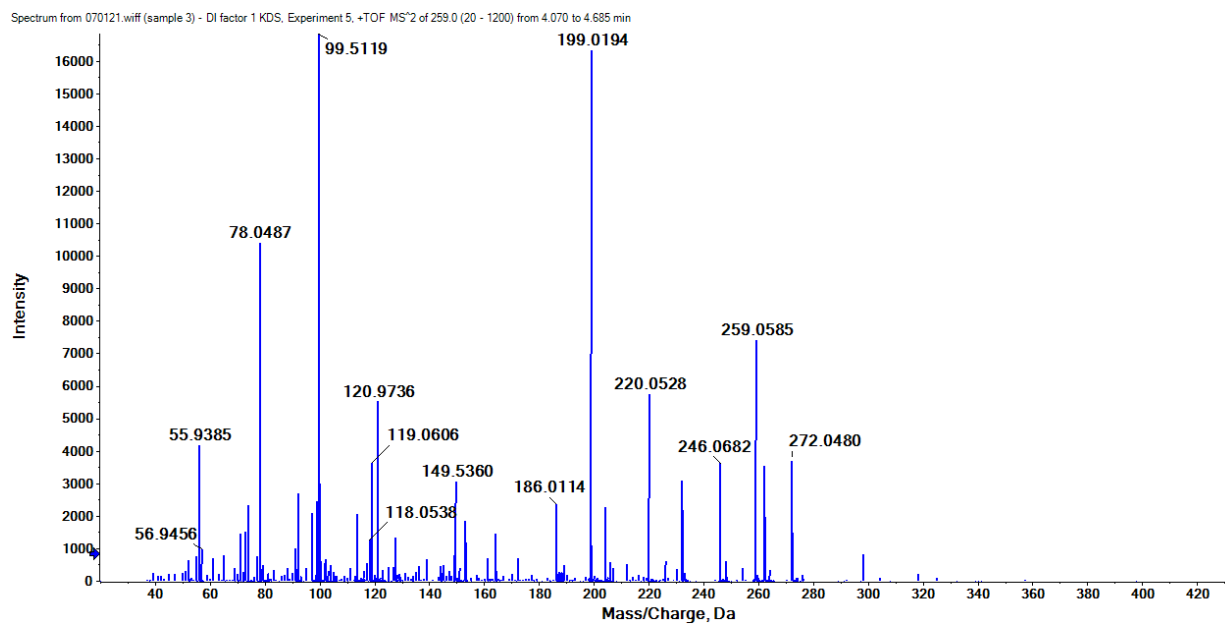
Fig. S21. Ion with m/z 199 in spectra (above) and ion current for described ion (below).

The 199 ion present is most likely explained by the composition: $[C_{11}H_{11}Fe]^+$. Similar MS-MS spectra were found for the ferrocenium-containing ion 259, which is a protonated ligand **11d** oxidized with respect to ferrocene.

m/z 259
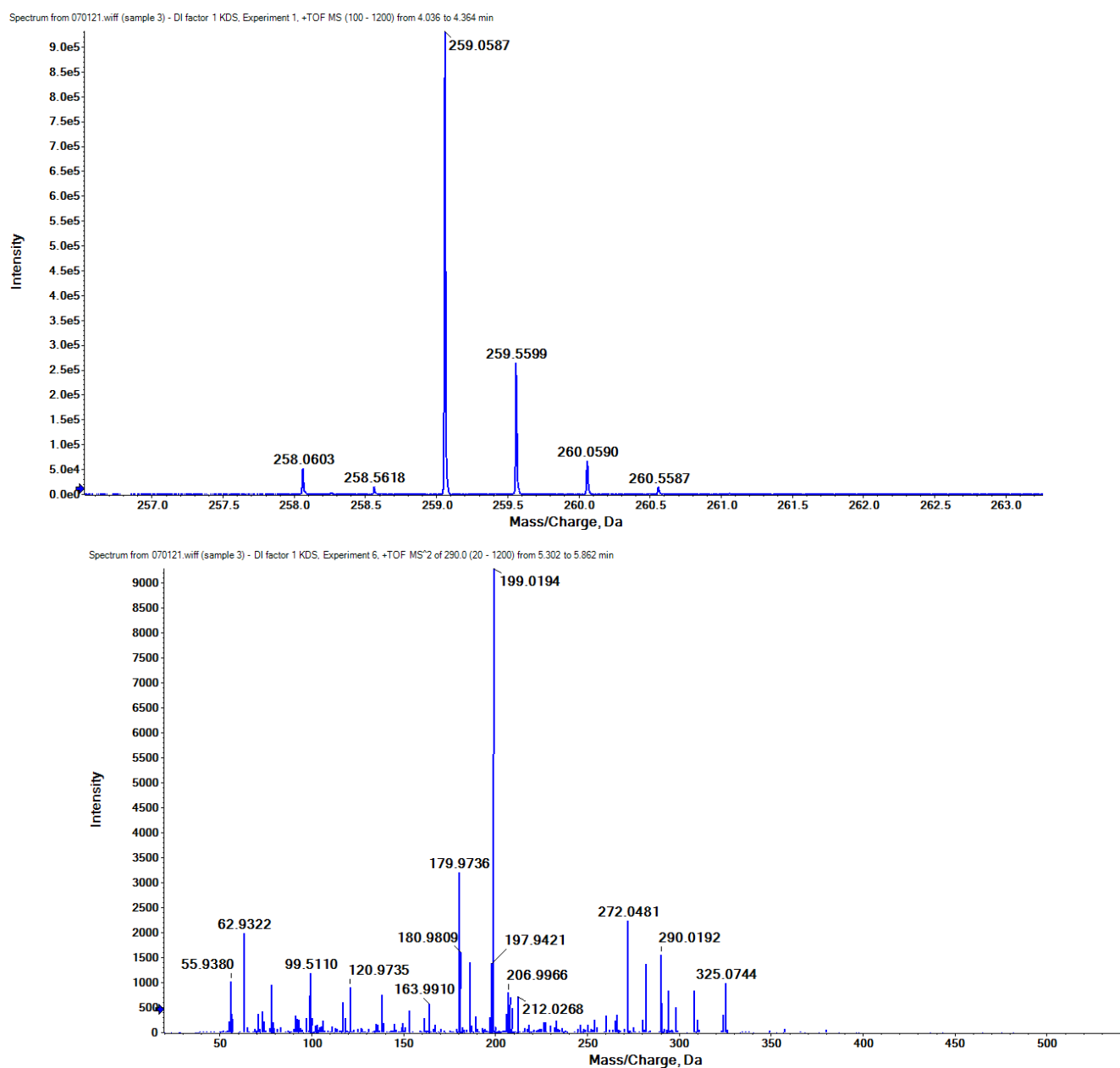
Fig. S22. Ion with m/z 259 in spectra (above) and it's MS-MS spectra (below).

Double-charged ion, Elemental composition $[C_{26}H_{28}FeN_3O_3S]^{2+}$, Delta -3.2 ppm.

Possible ion structure is = $[DG-605-Fe^{3+}+H^+]^{2+}$

6. MTT Assay

The measurements were carried out using the standard MTT method. 2500 cells per well for MCF7, HEK293T were plated out in 135 µl of DMEM-F12 media (Gibco) in 96-well plate and incubated in the 5% CO_2 incubator for first 16 h with out treating. Then 15 µl of media-DMSO solutions of tested substances to the cells (final DMSO concentrations in the media were 1% or less) and treated cells 72 h with 50 nM-100 µM (eight dilutions) of our substances (triplicate each). The MTT reagent then was added to cells up to final concentration of 0.5 g/l (10X stock solution in PBS was used) and incubated for 2 h at 37ºC in the incubator, under an atmosphere of 5% CO_2. The MTT solution was then discarded and 140 µl of DMSO was added. The plates were swayed on a shaker (60 rpm) to solubilize the formazan. The absorbance was measured using a microplate reader (VICTORX5 Plate Reader) at a wavelength of 565 nm (in order to measure formazan concentration). The results were used to construct a dose-response graph and to estimate CC_{50} value (GraphPad Software, Inc.). All measurements were reproduced in two bio-replicas to averaging the obtained data and calculating the IC_{50} values.

7. NMR and IR Spectra of synthesized compounds
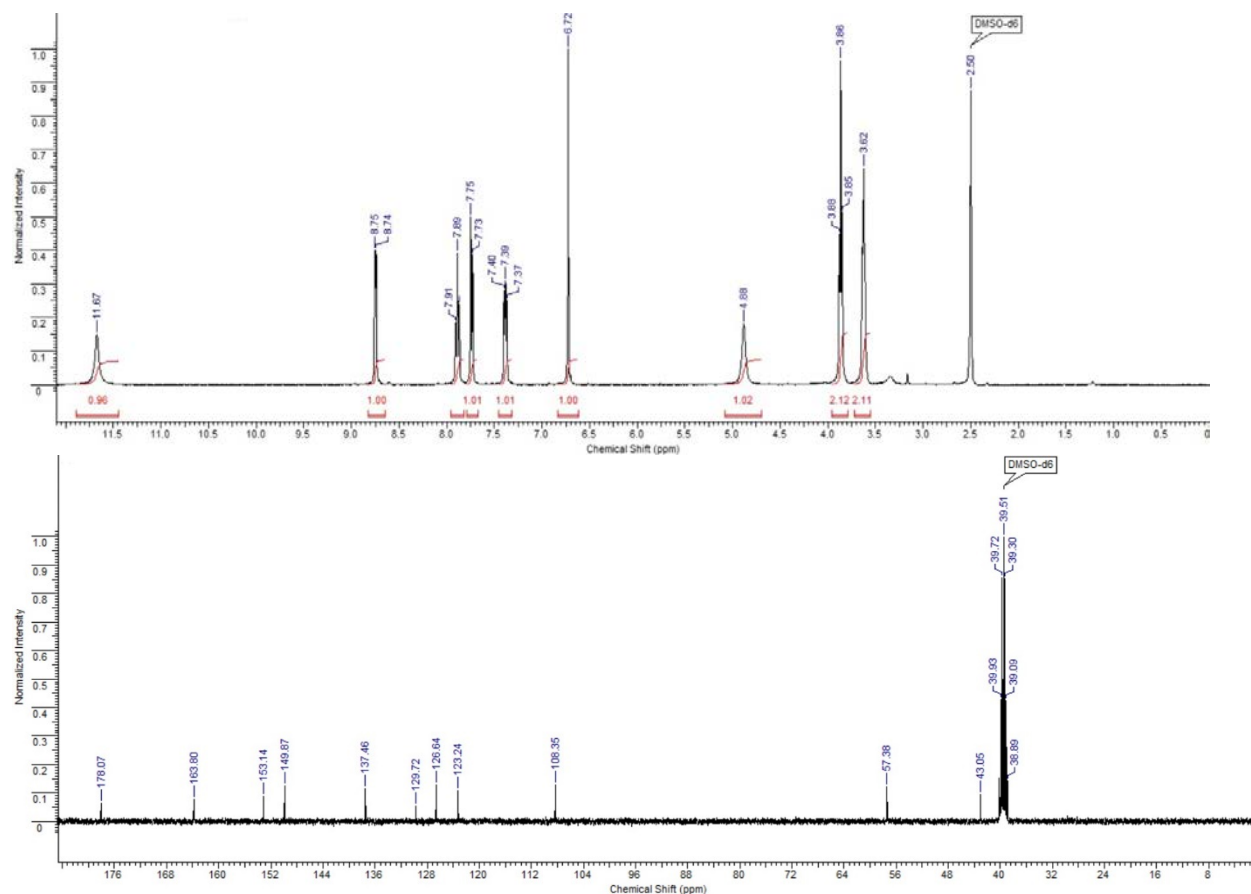
Fig. S23. ^{1}H, ^{13}C NMR for compound **1**.
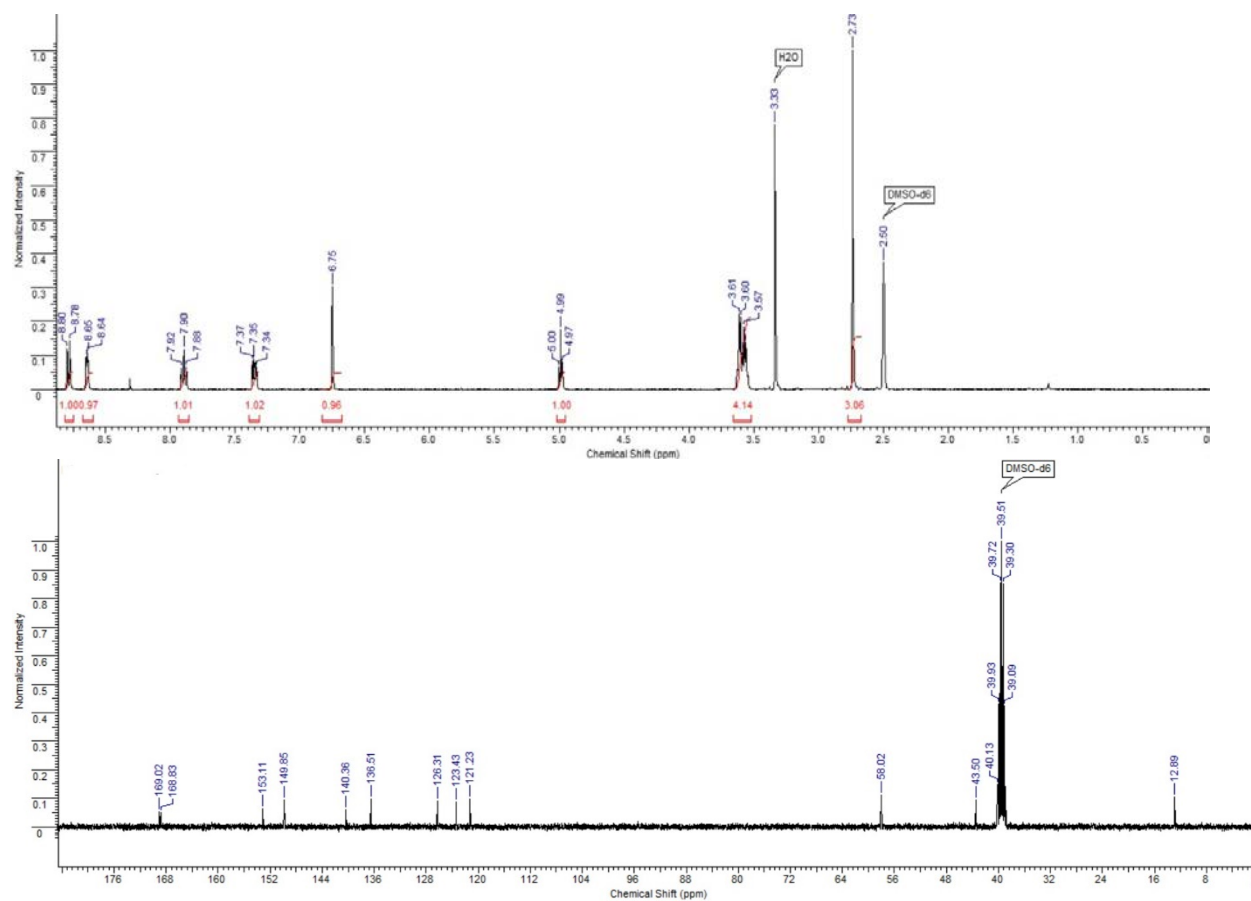
Fig. S24. ^{1}H, ^{13}C NMR for compound **2**.
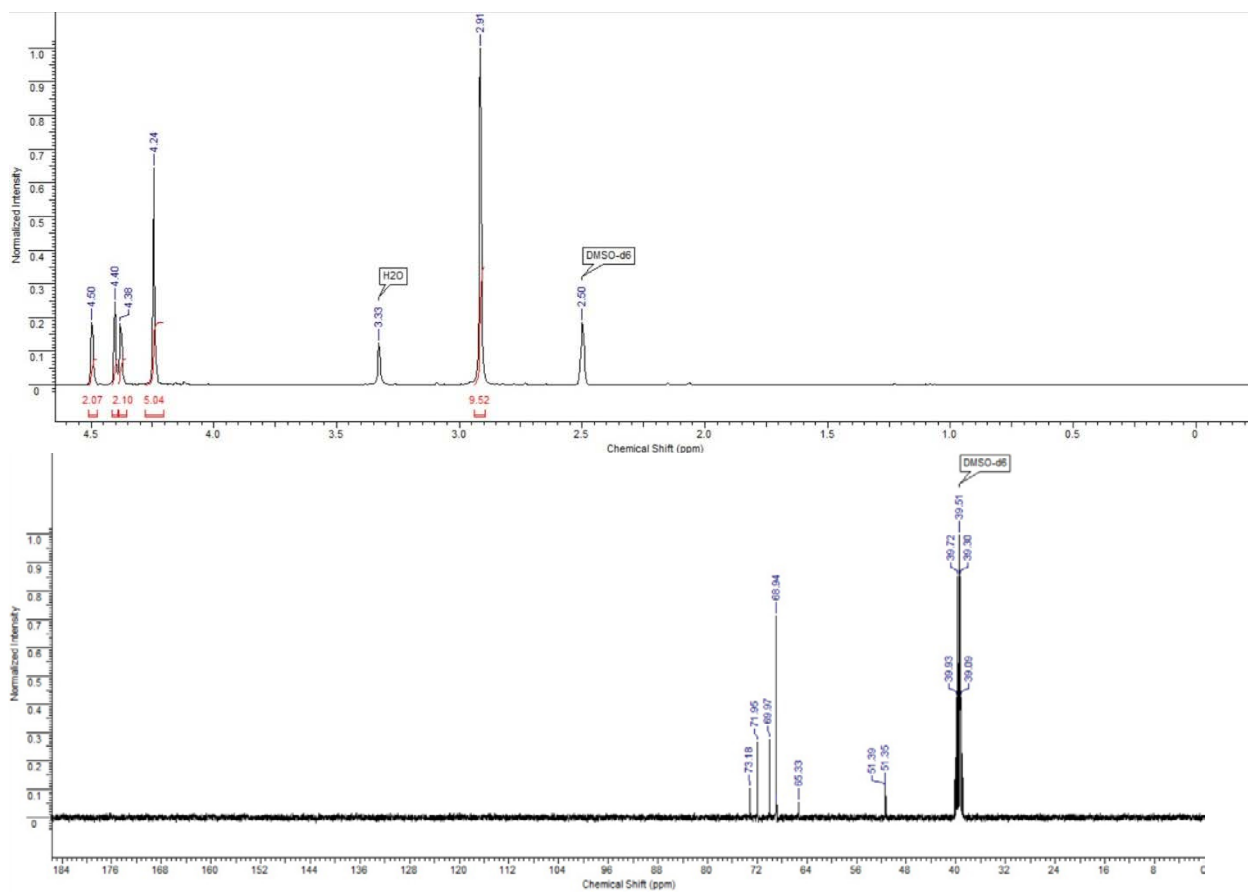
Fig. S25. ^{1}H, ^{13}C NMR for compound **4**.
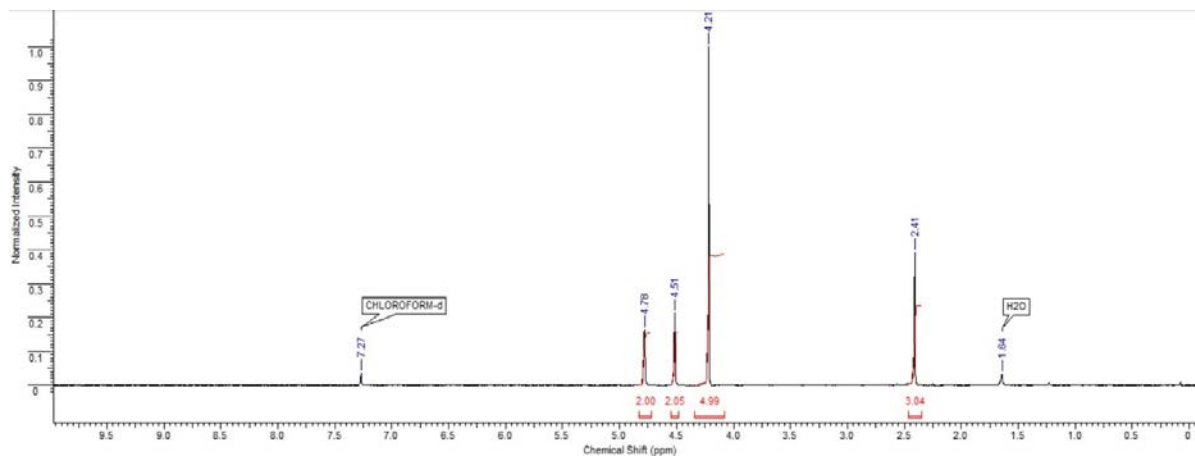
Fig. S26. ^{1}H NMR for compound **6**.
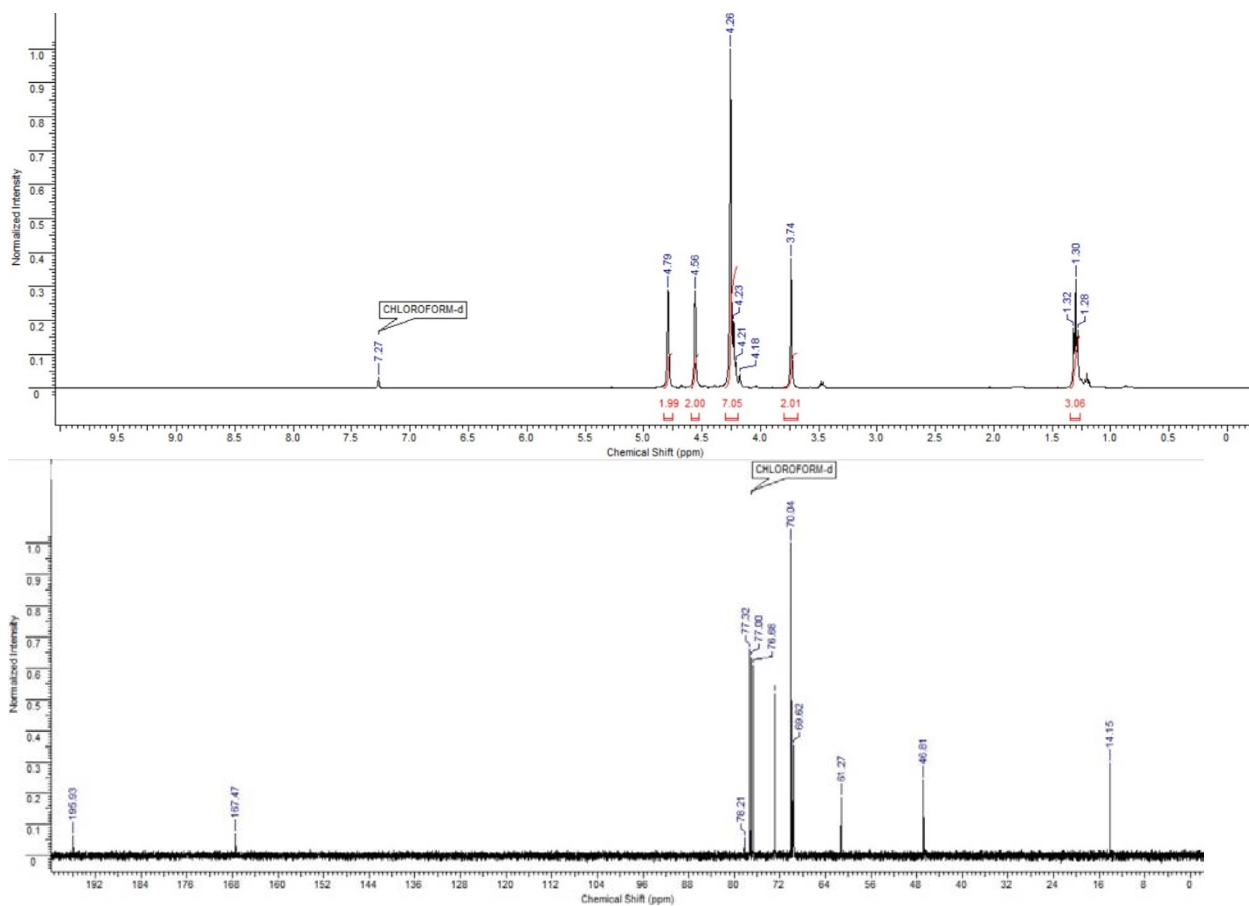
Fig. S27. ^{1}H, ^{13}C NMR for compound **7**.
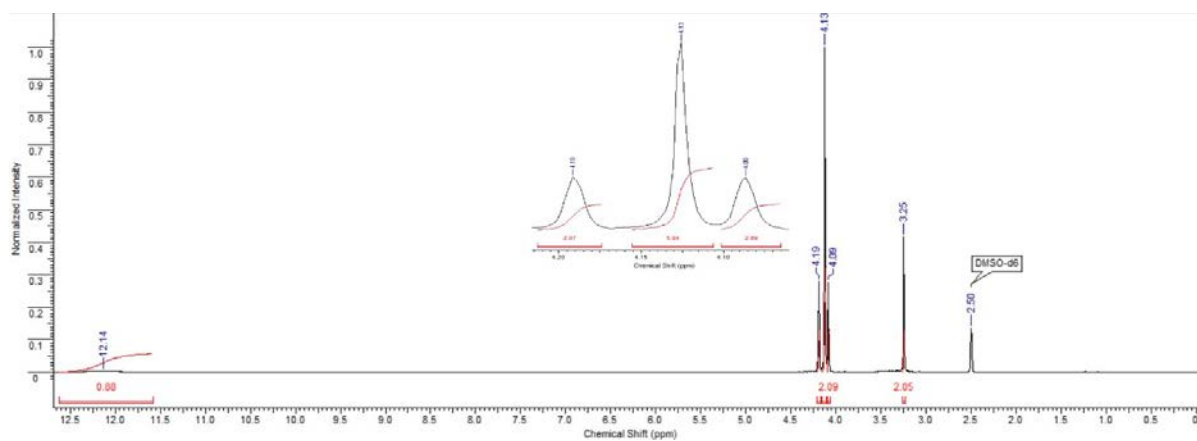
Fig. S28. ^{1}H NMR for compound **8**.
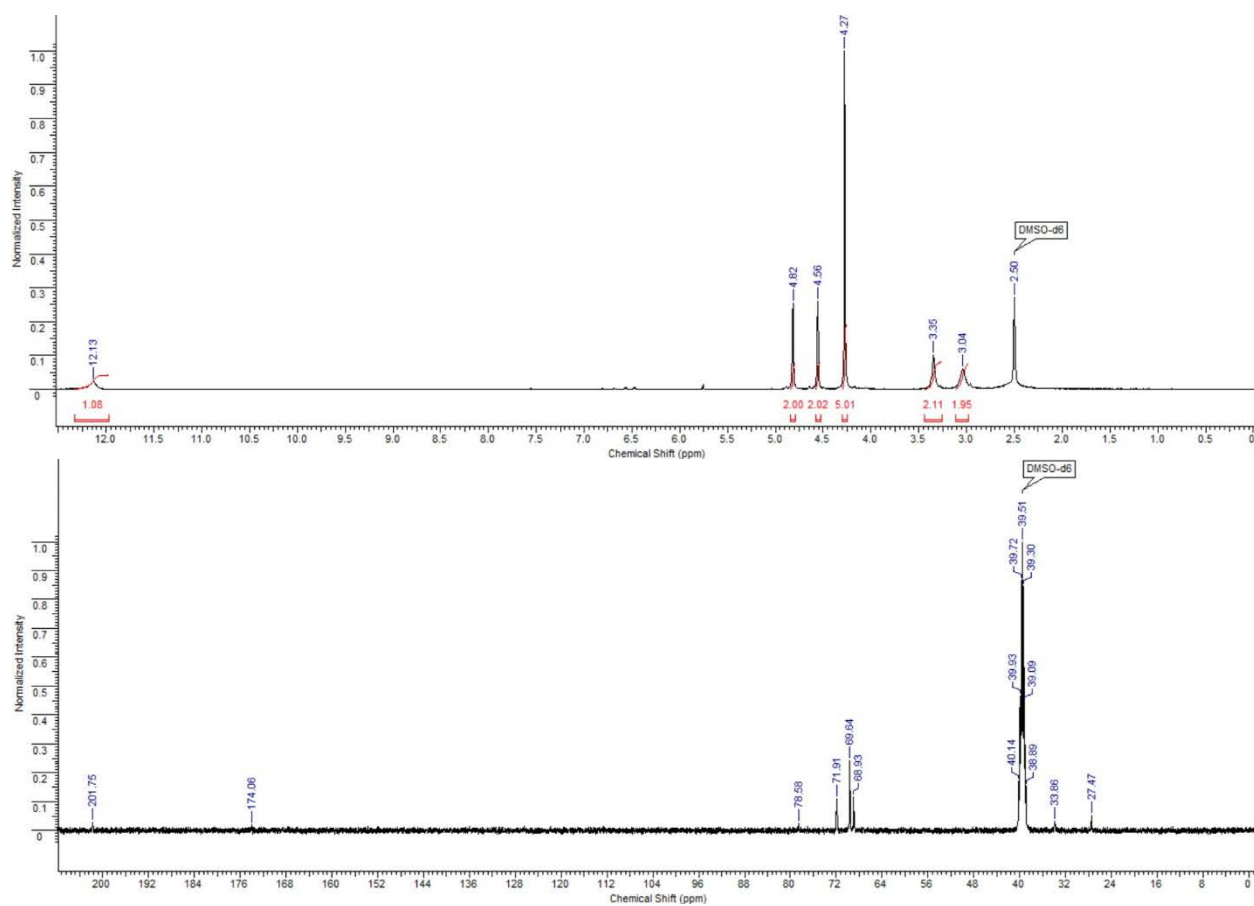
Fig. S29. ^{1}H, ^{13}C NMR for compound **9**.
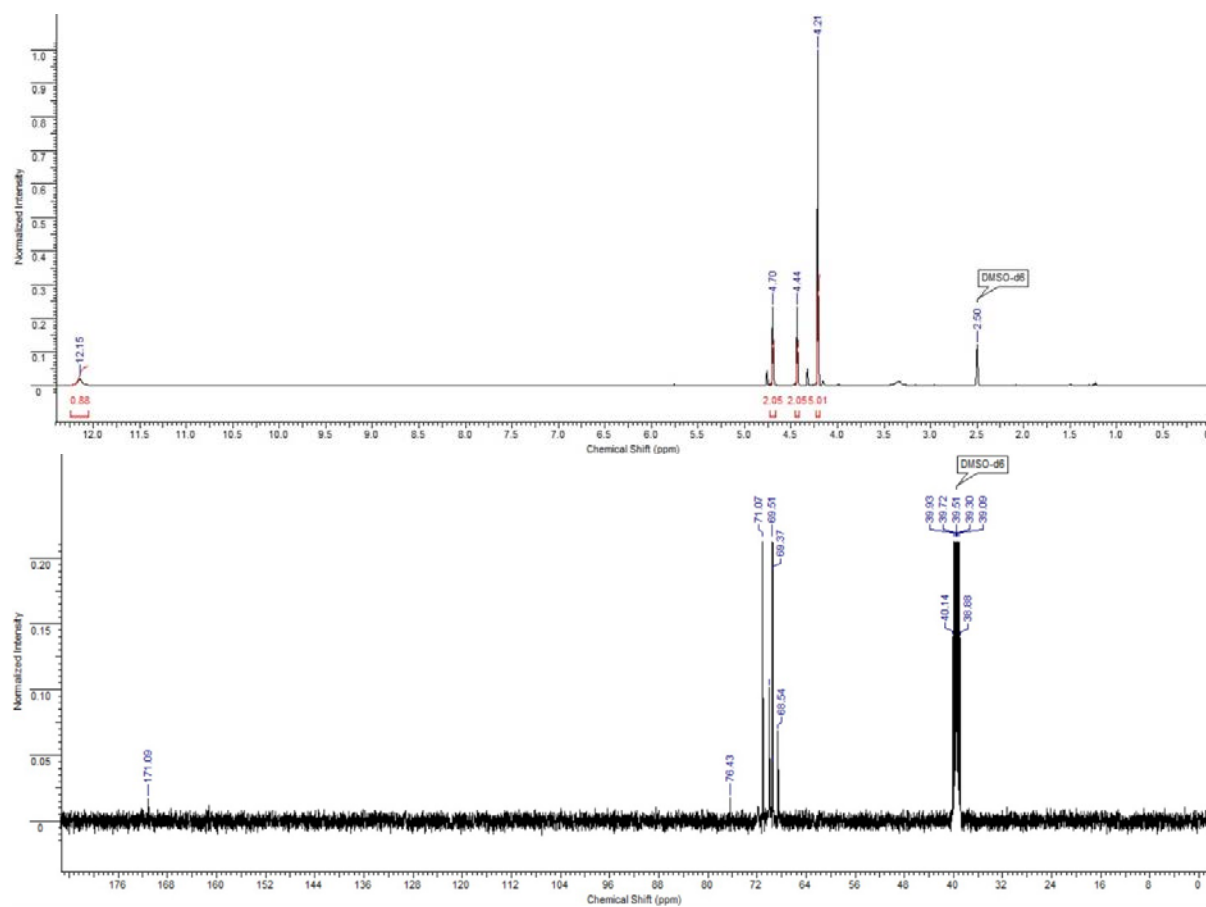
Fig. S30. ^{1}H, ^{13}C NMR for compound **3a**.
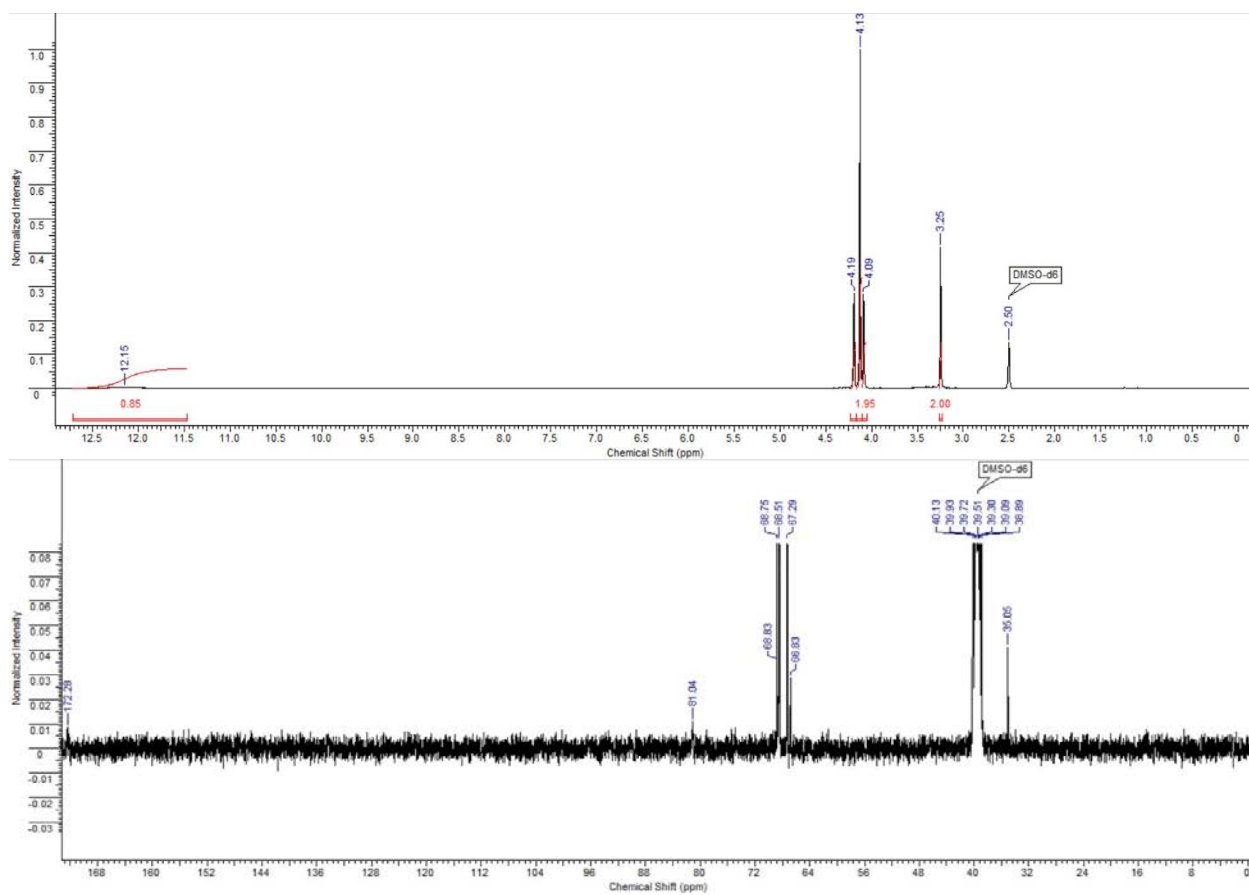
Fig. S31. ¹H, ¹³C NMR for compound **3b**.
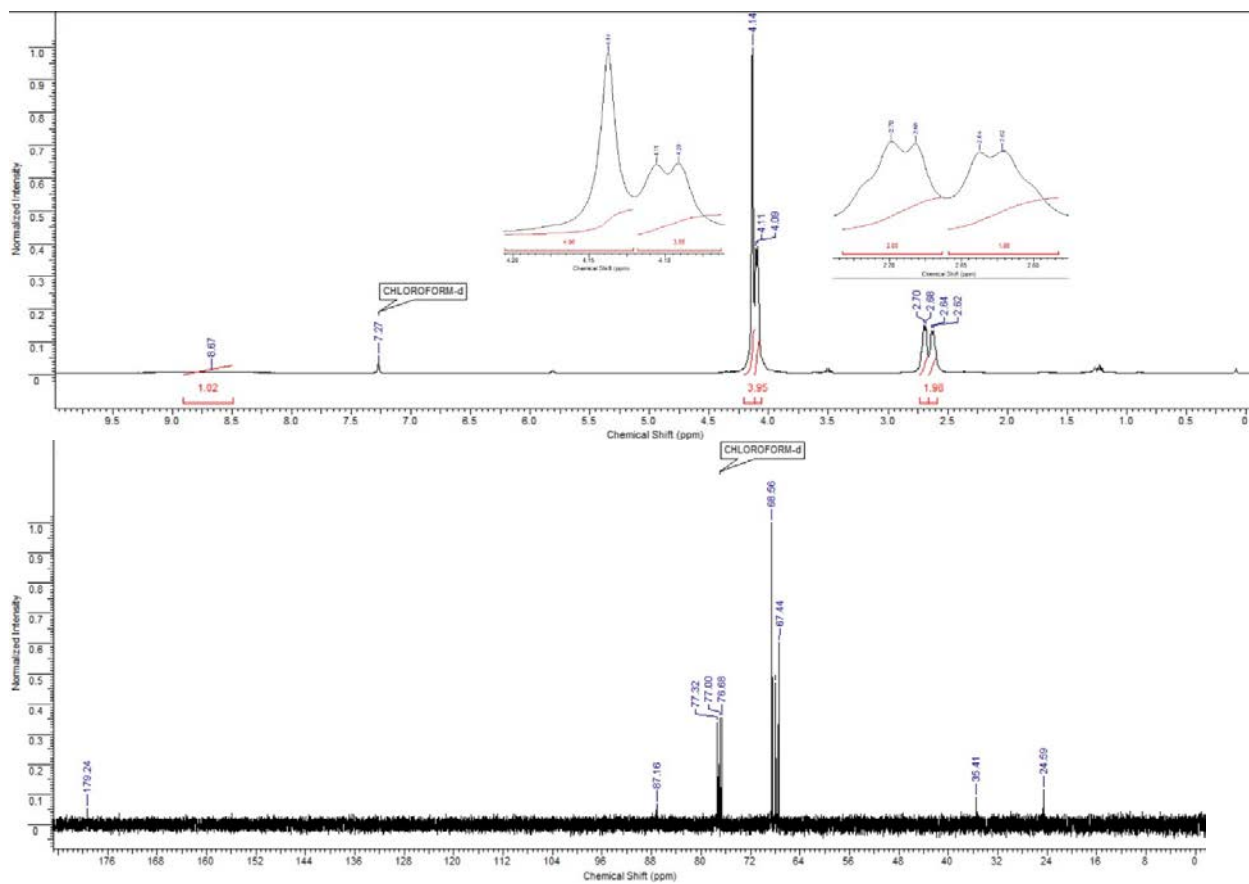
Fig. S32. ¹H, ¹³C NMR for compound **3c**.
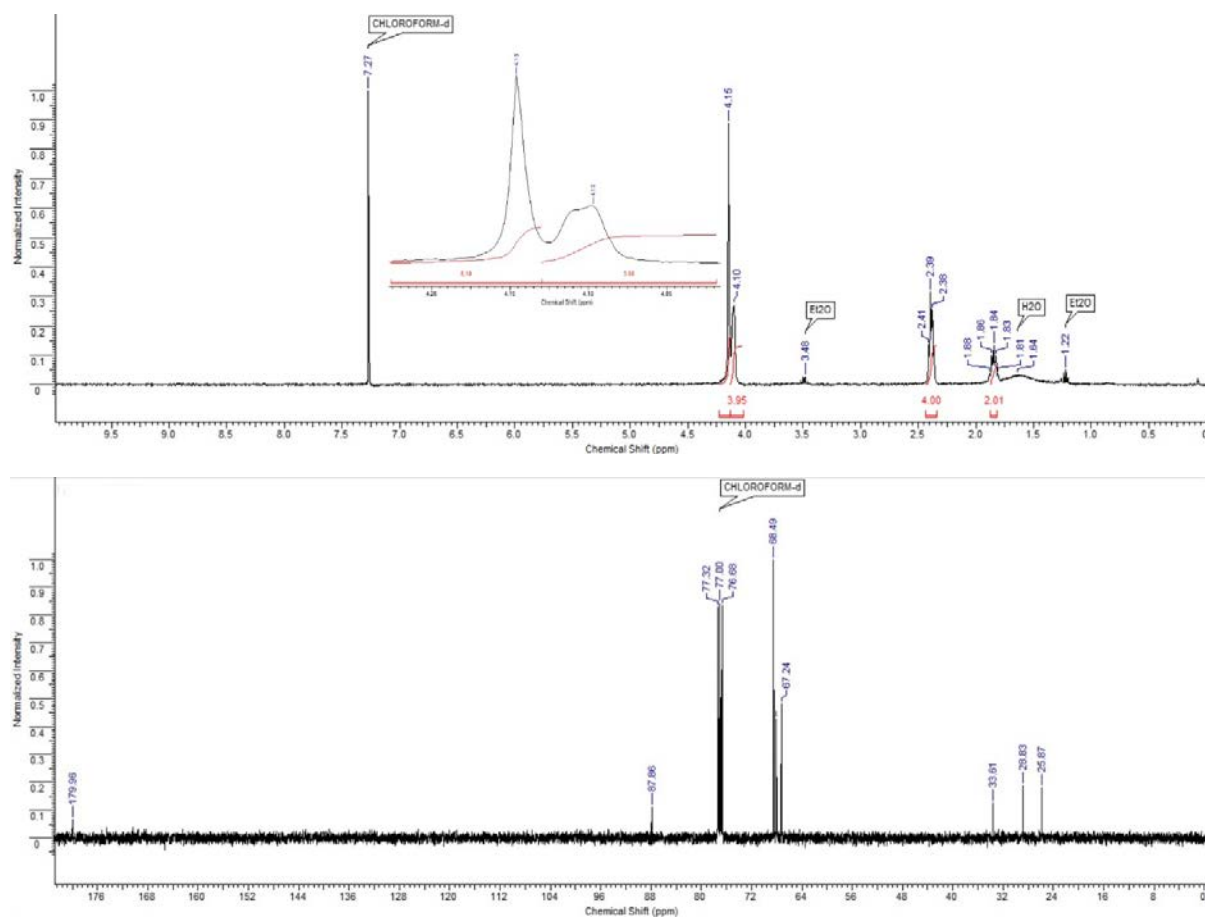
Fig. S33. ^{1}H, ^{13}C NMR for compound **3d**.
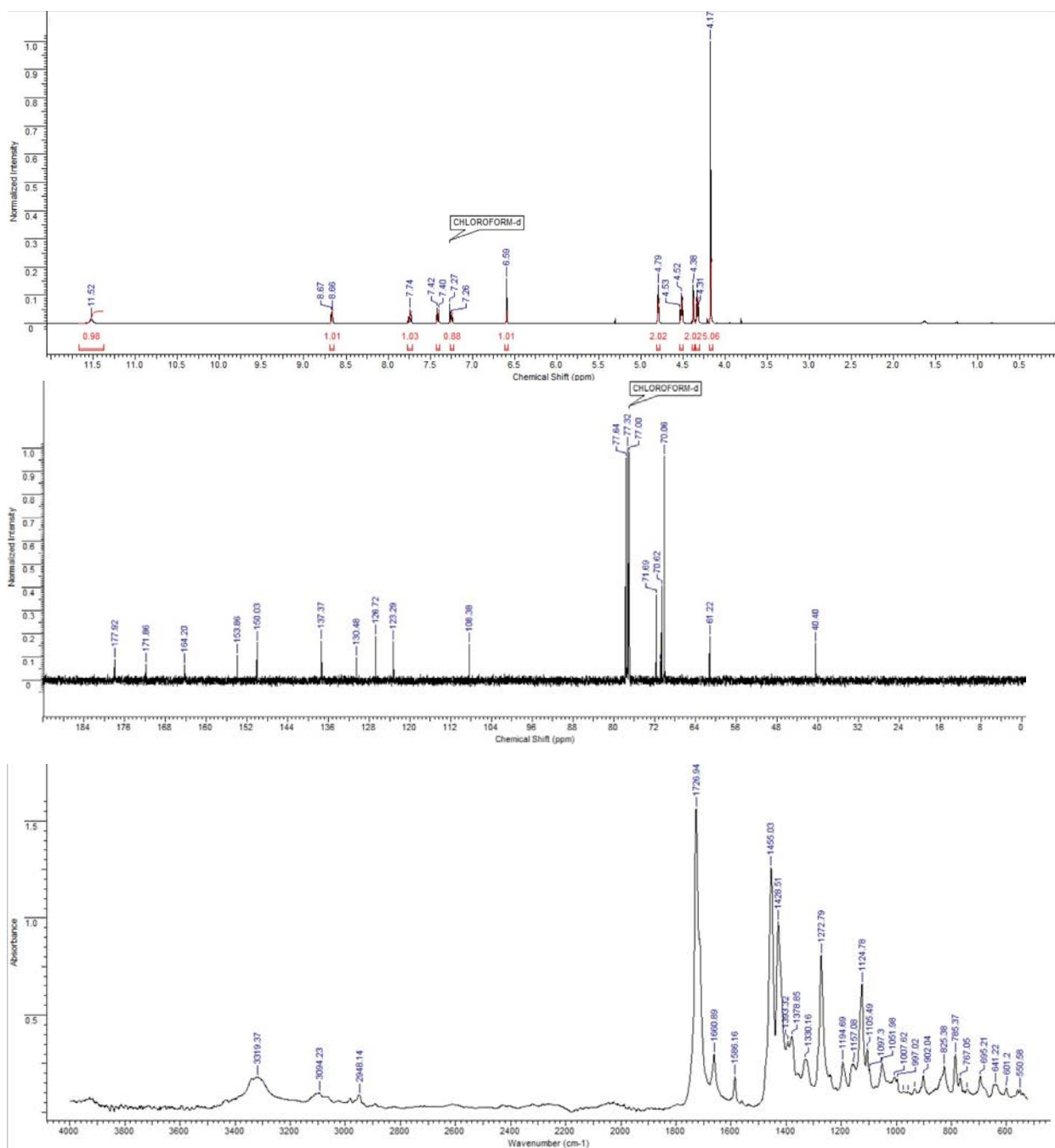
Fig. S34. ^{1}H, ^{13}C NMR, IR for compound **10a**.
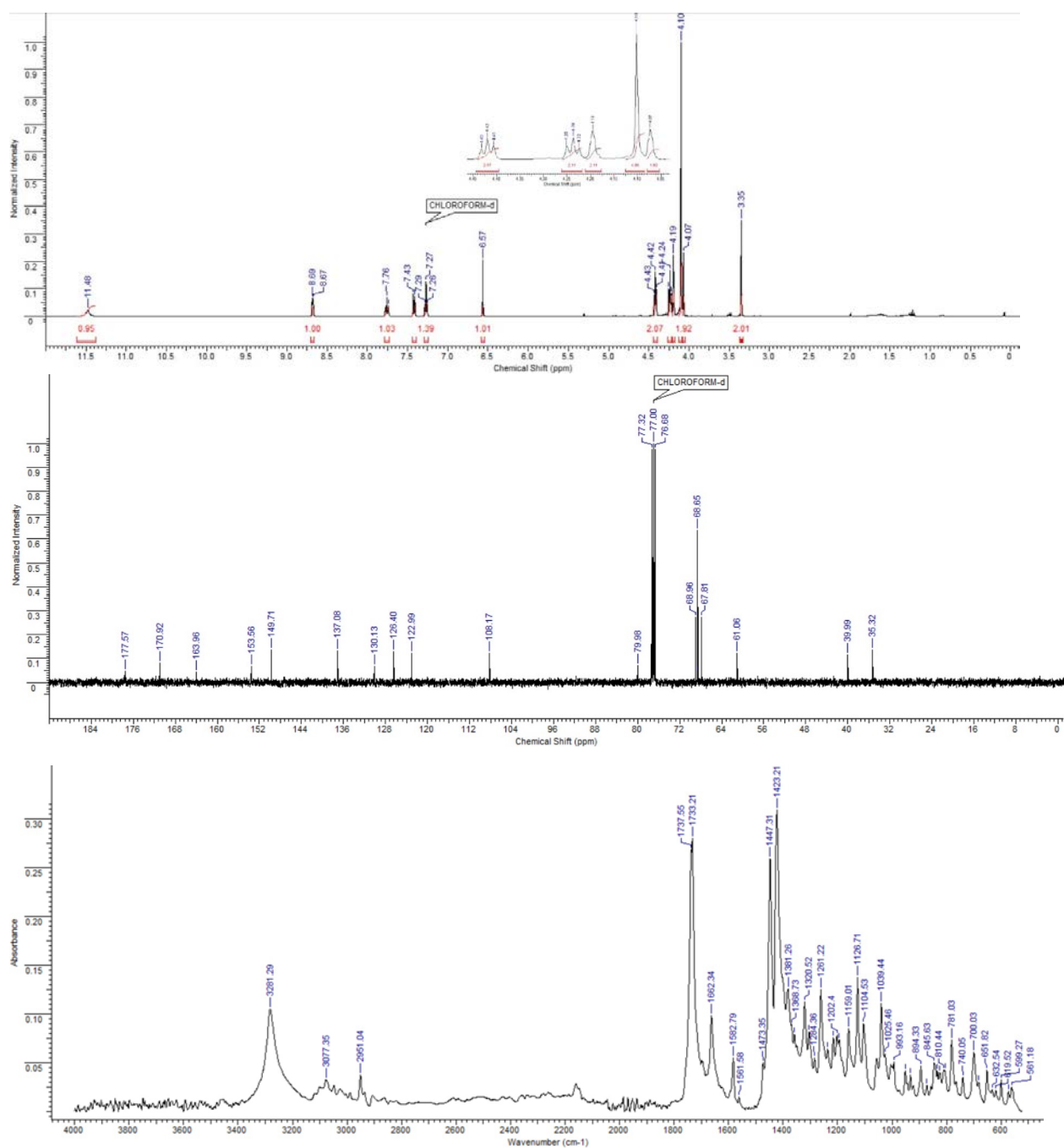
Fig. S35. ^{1}H, ^{13}C NMR, IR for compound **10b**.
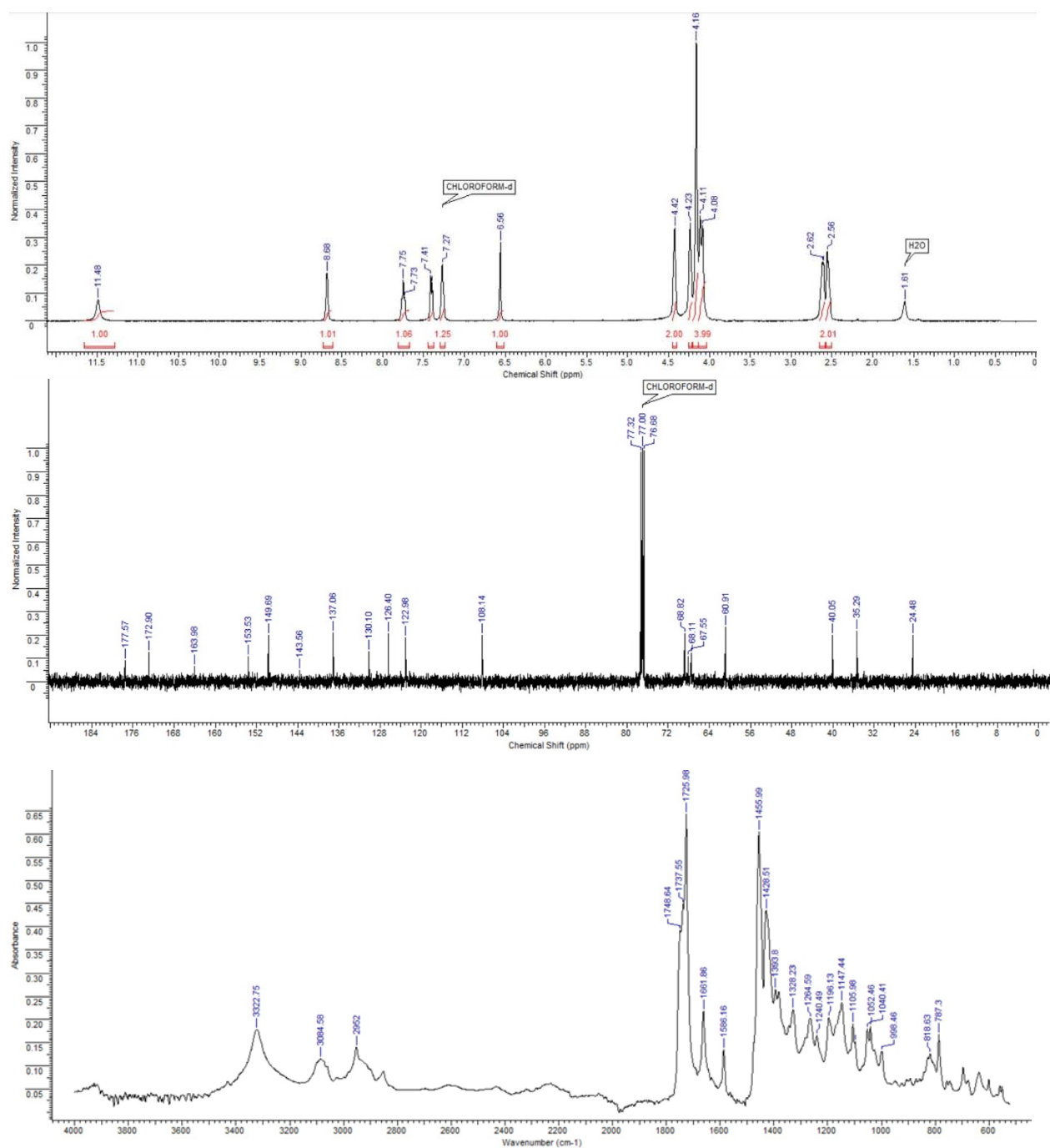
Fig. S36. ^{1}H, ^{13}C NMR, IR for compound **10c**.
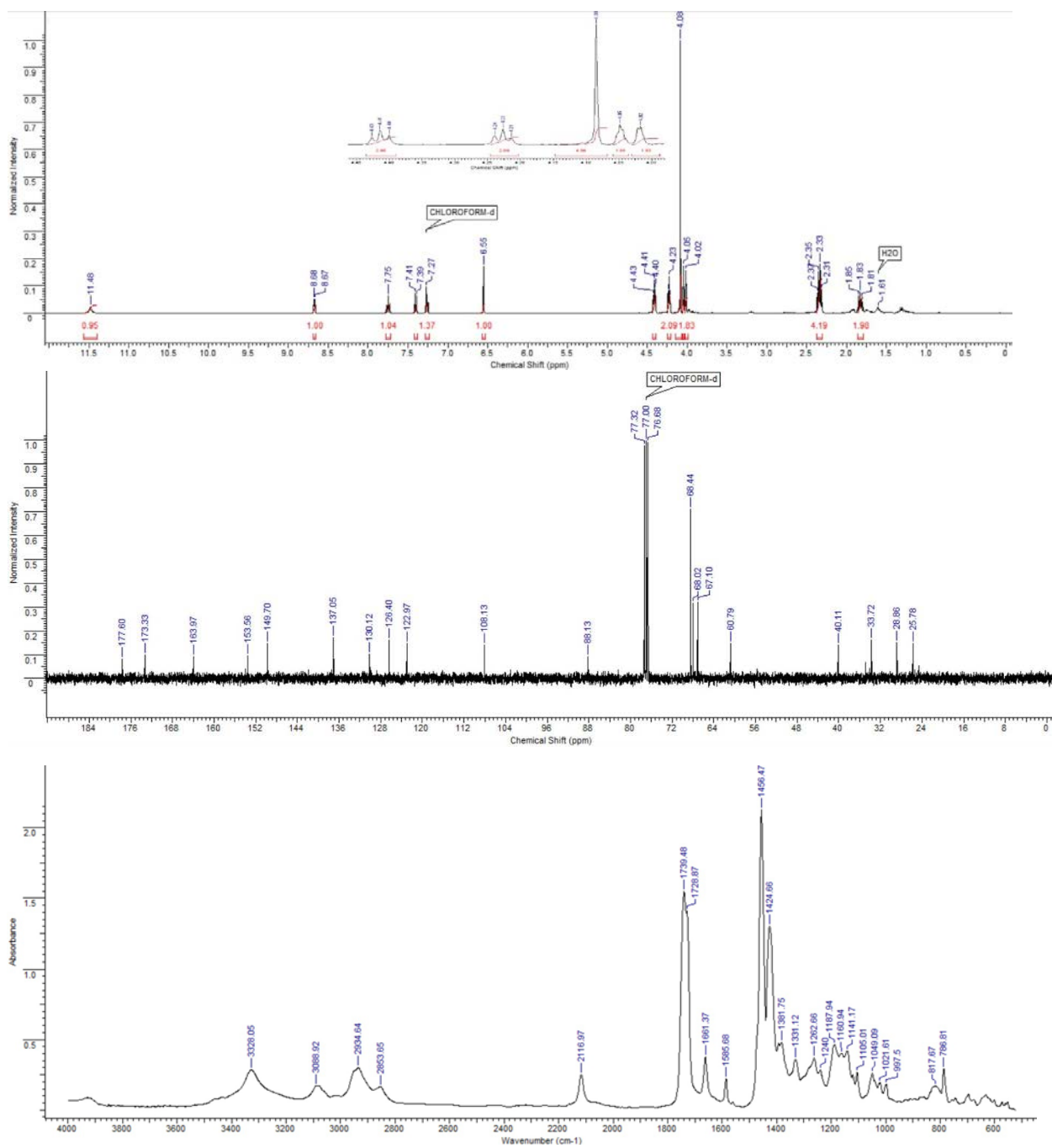
Fig. S37. ^{1}H, ^{13}C NMR, IR for compound **10d**.
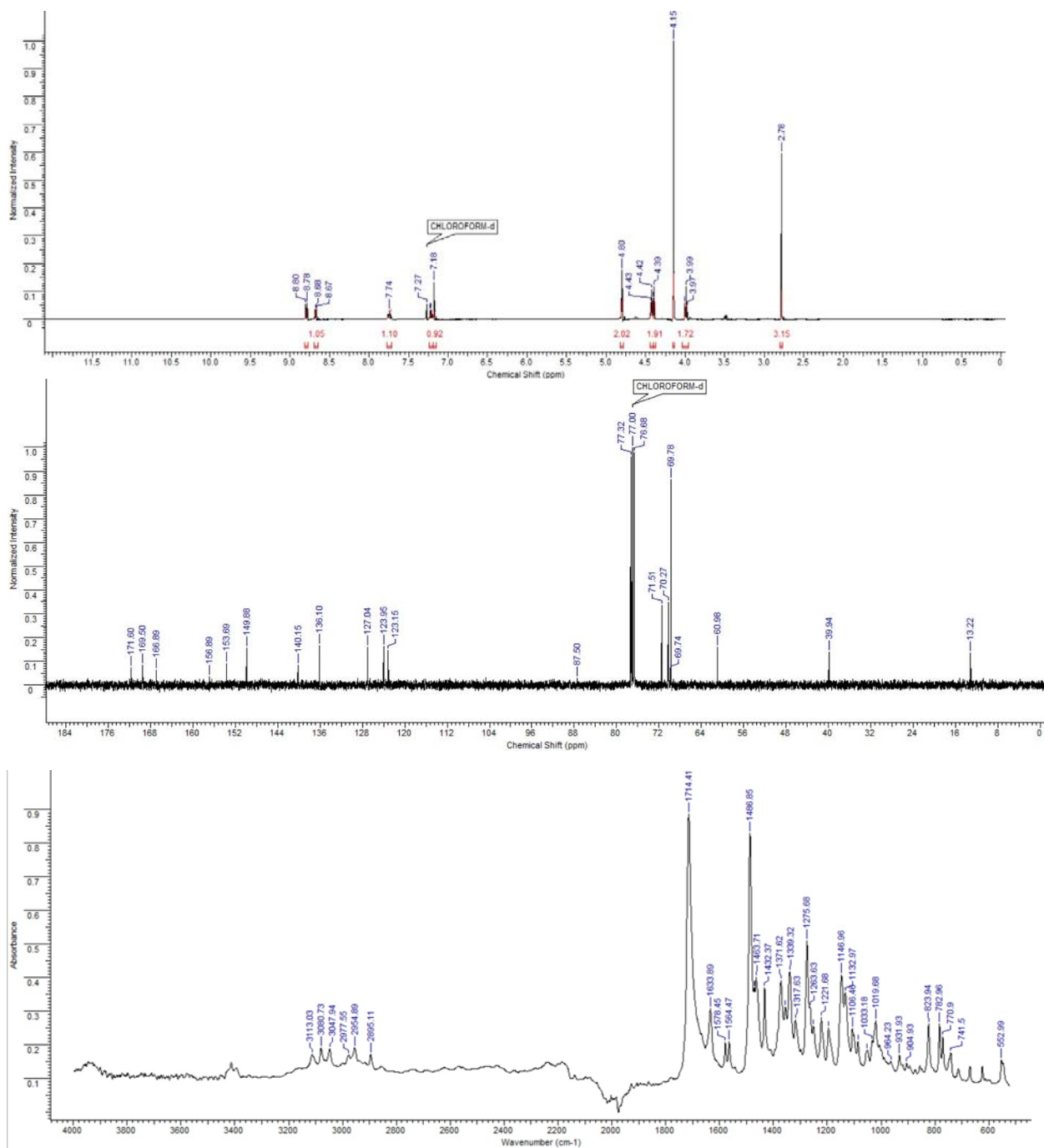
Fig. S38. ^{1}H, ^{13}C NMR, IR for compound **11a**.
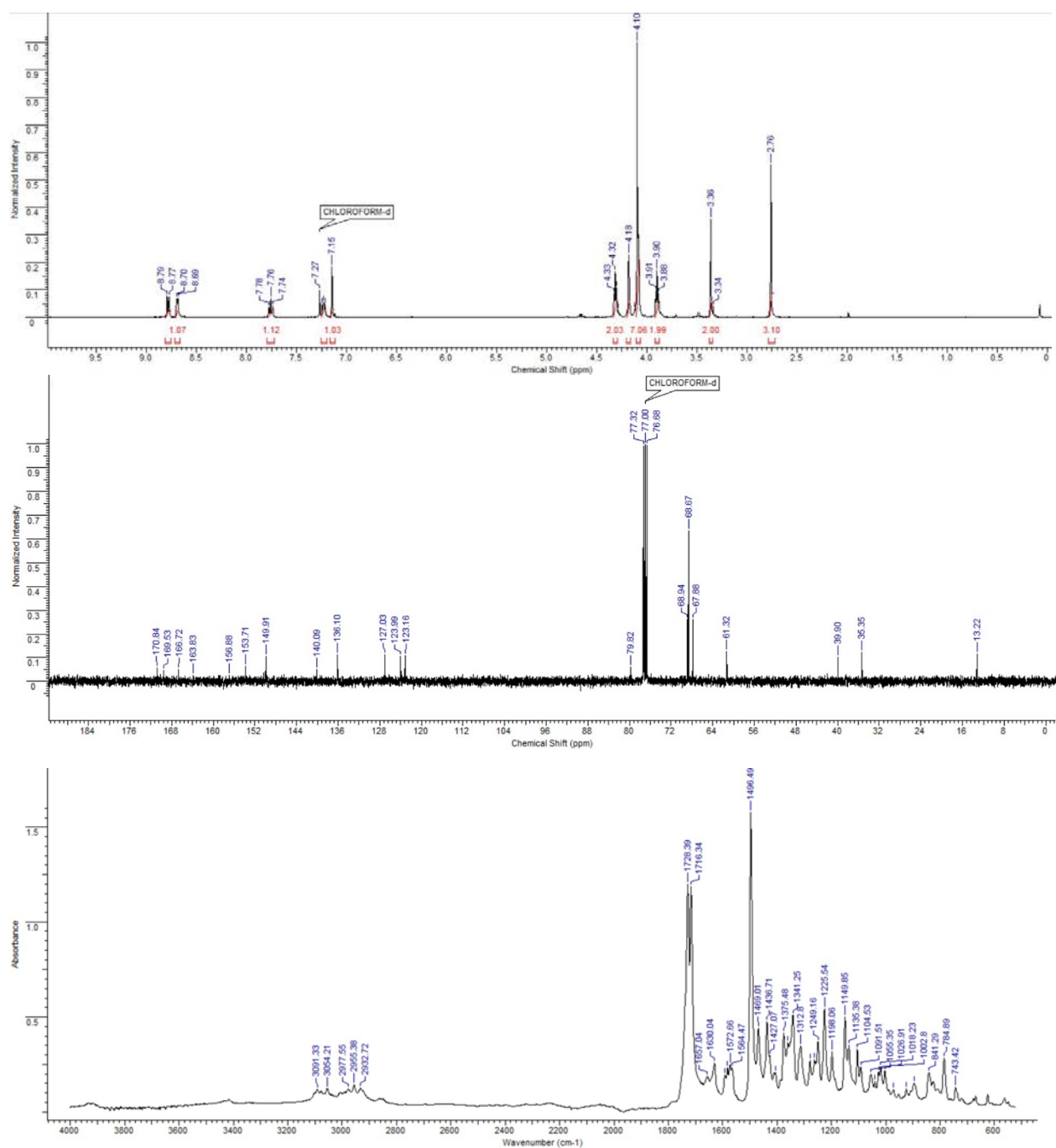
Fig. S39. ^{1}H, ^{13}C NMR, IR for compound **11b**.
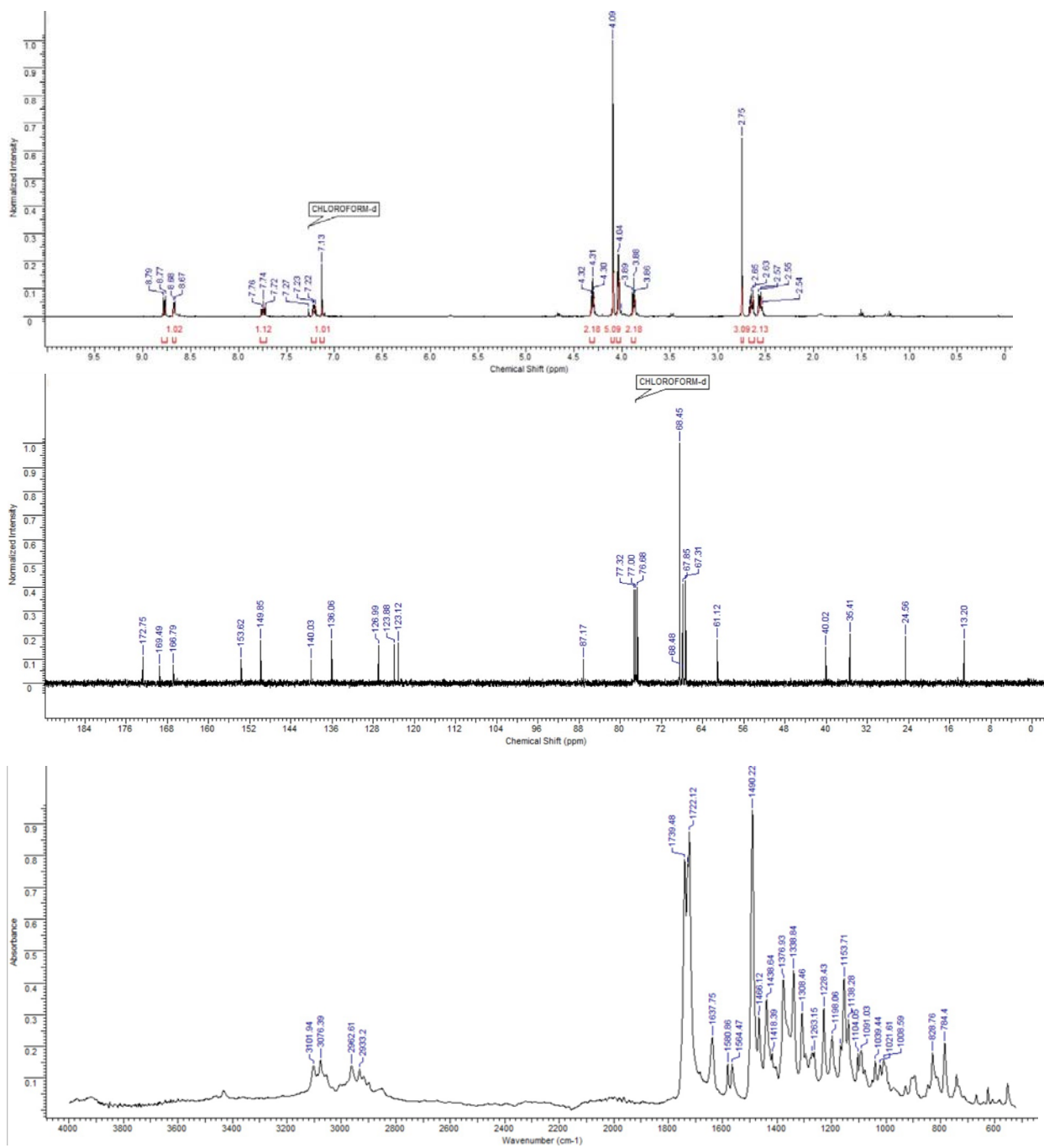
Fig. S40. ^{1}H, ^{13}C NMR, IR for compound **11c**.
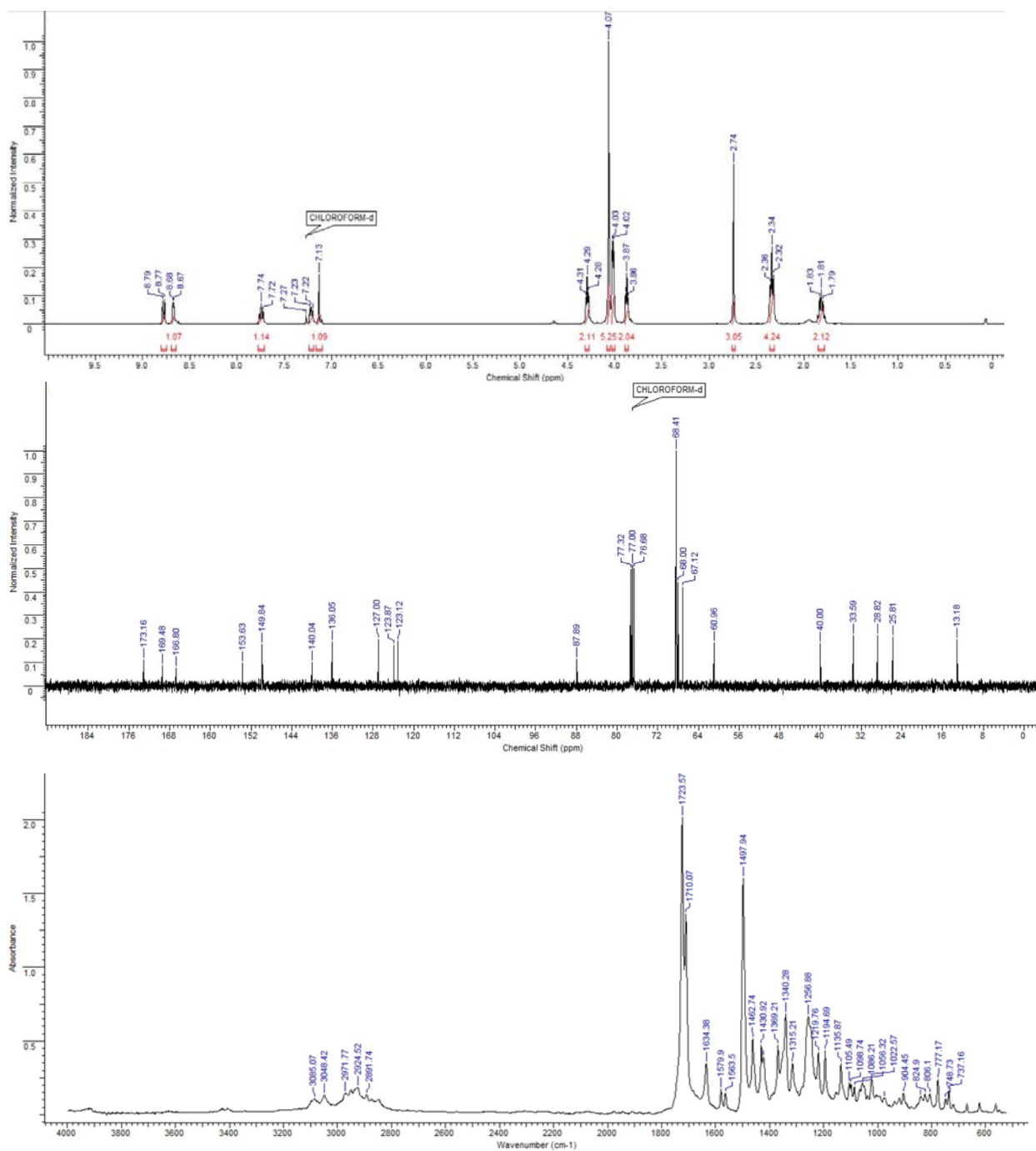
Fig. S41. ^{1}H, ^{13}C NMR, IR for compound **11d**.
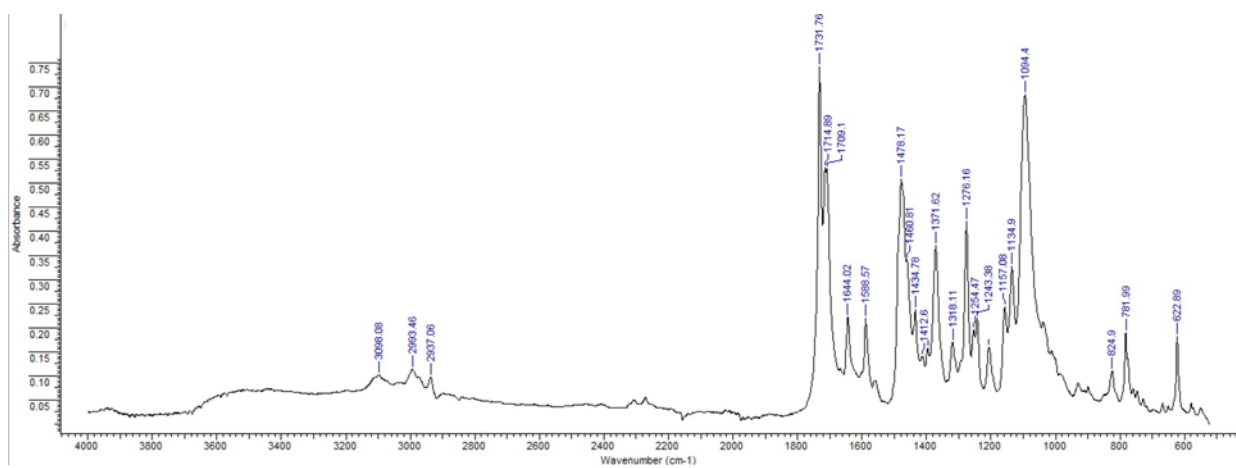
Fig. S42. IR for compound **12a**.
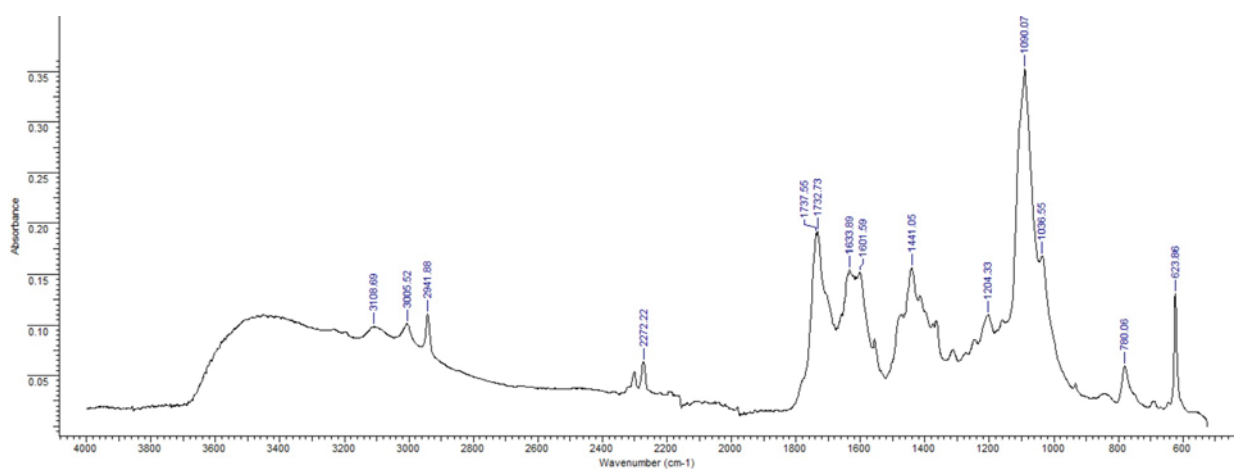
Fig. S43. IR for compound **12b**.
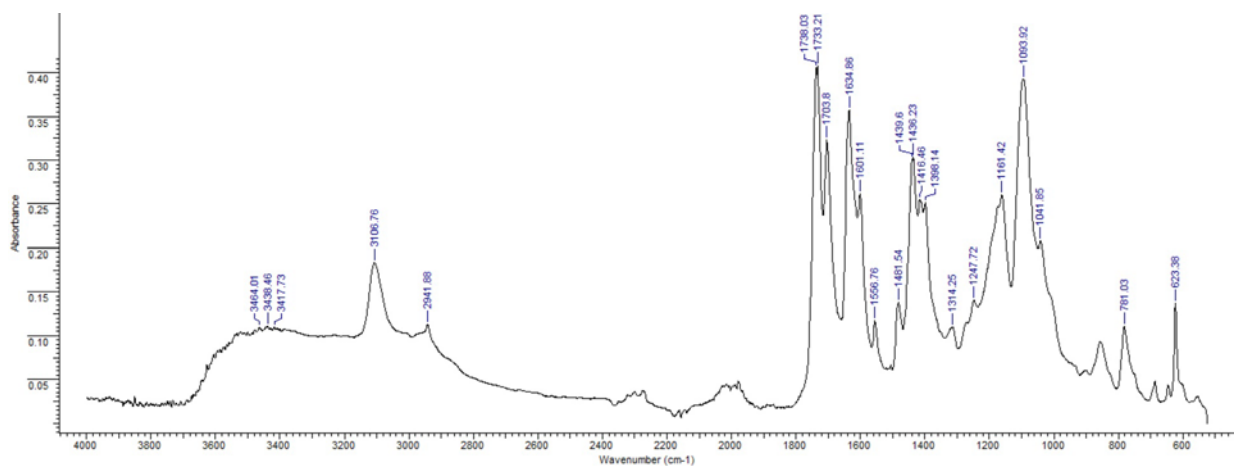
Fig. S44. IR for compound **12c**.
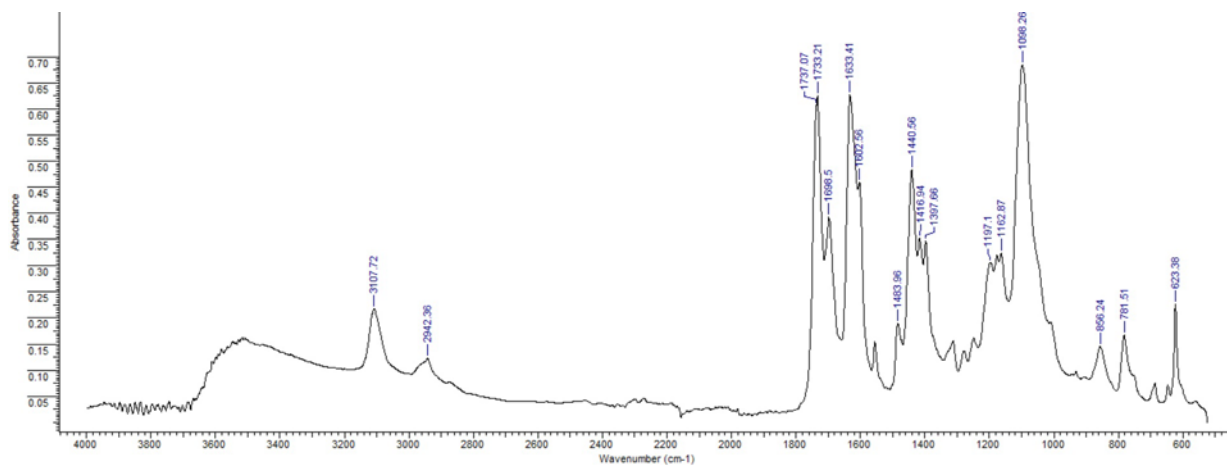
Fig. S45. IR for compound **12d**.
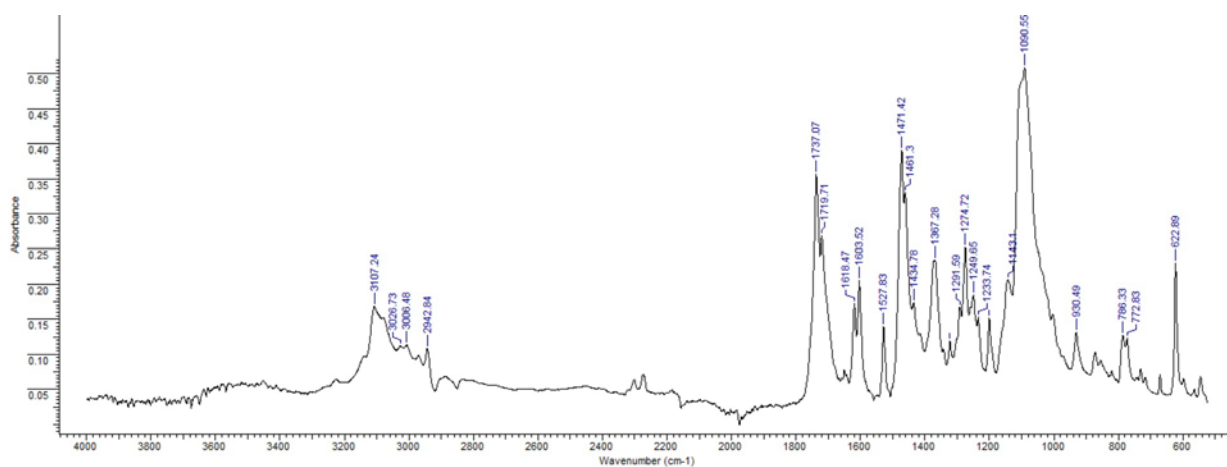
Fig. S46. IR for compound **13a**.
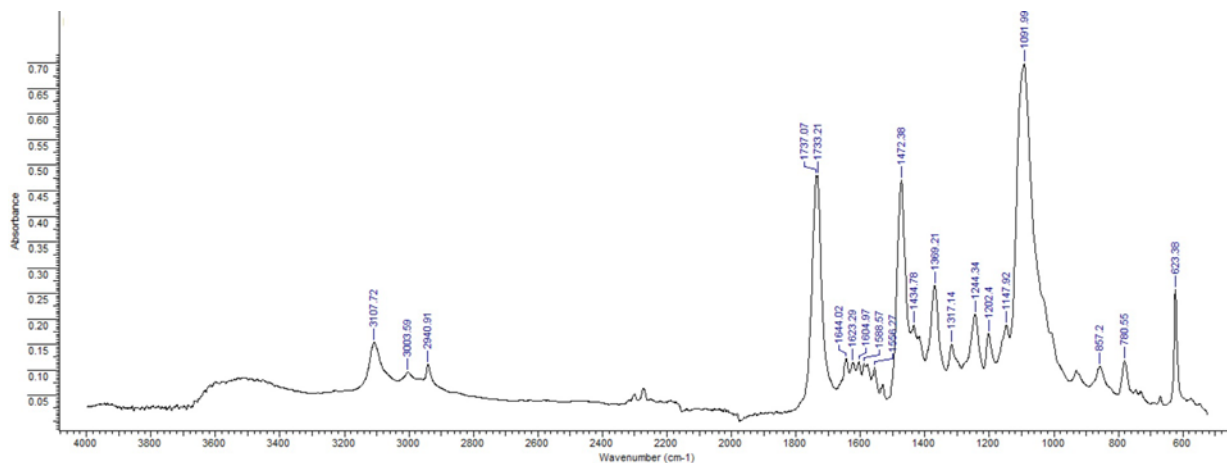
Fig. S47. IR for compound **13b**.
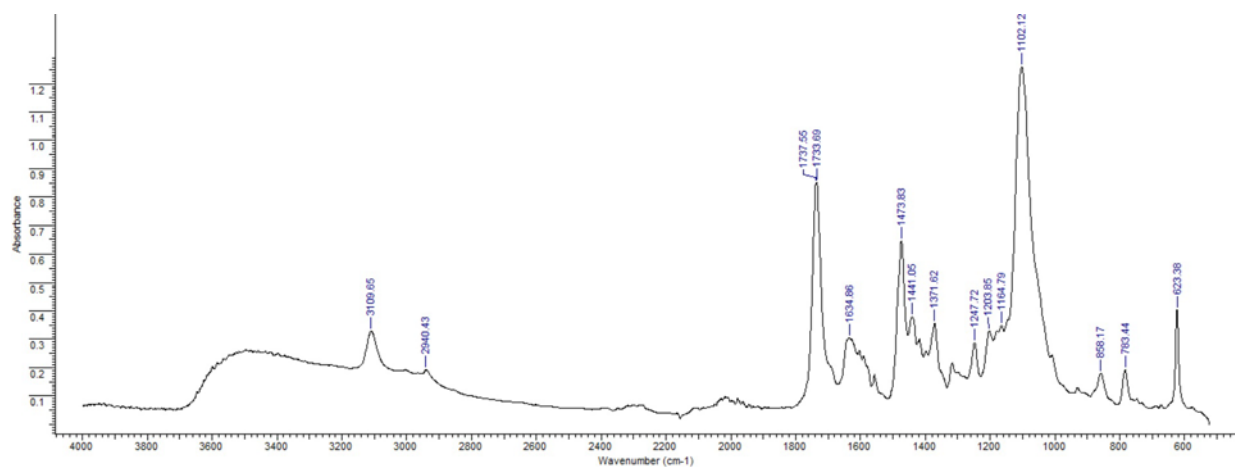
Fig. S48. IR for compound **13c**.
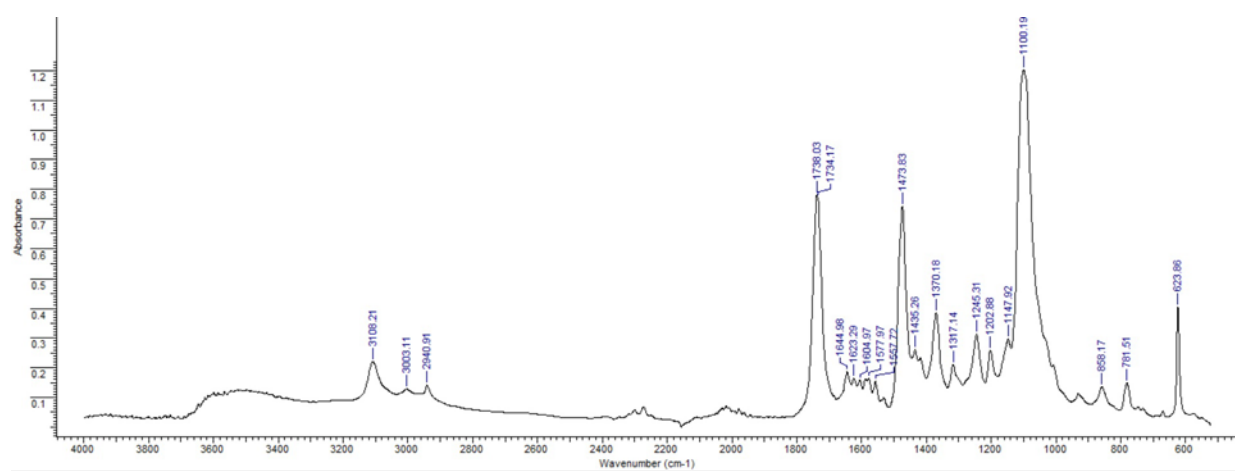
Fig. S49. IR for compound **13d**.
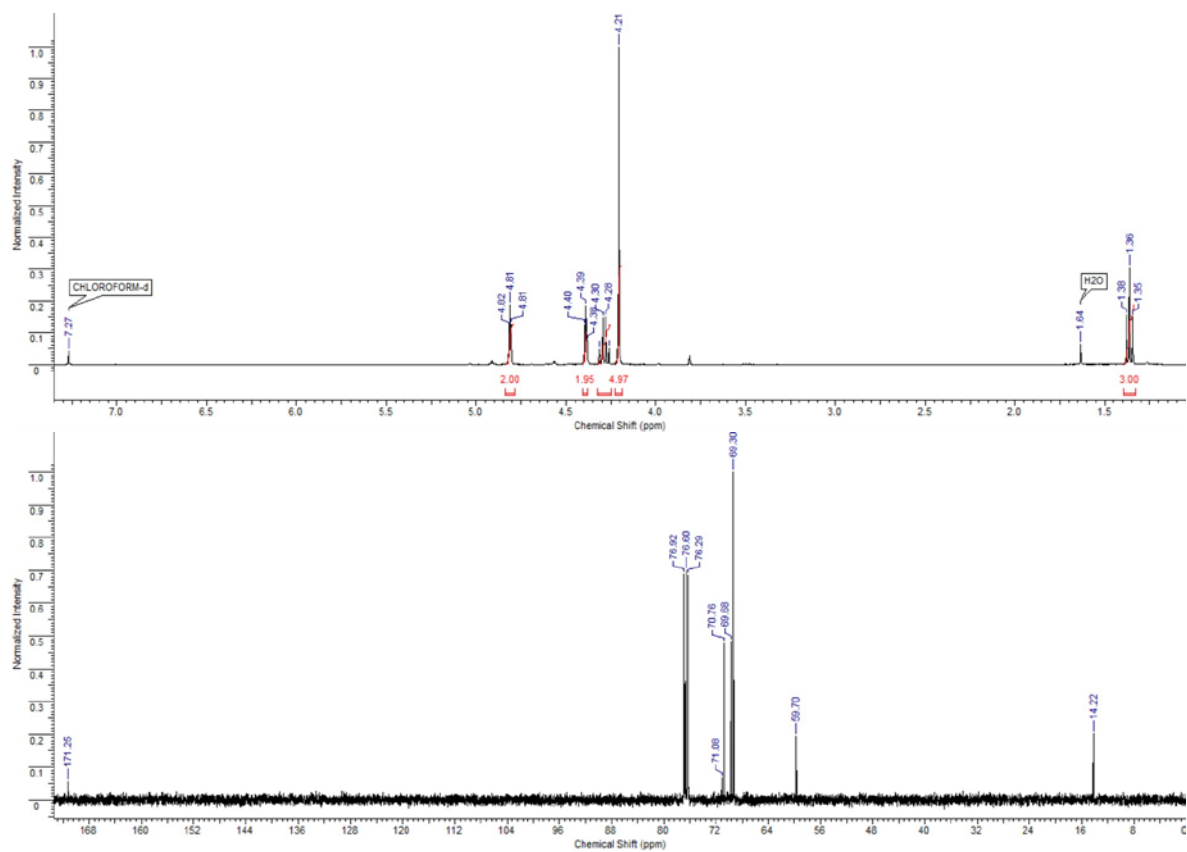
Fig. S50. ¹H, ¹³C NMR for compound **14**.
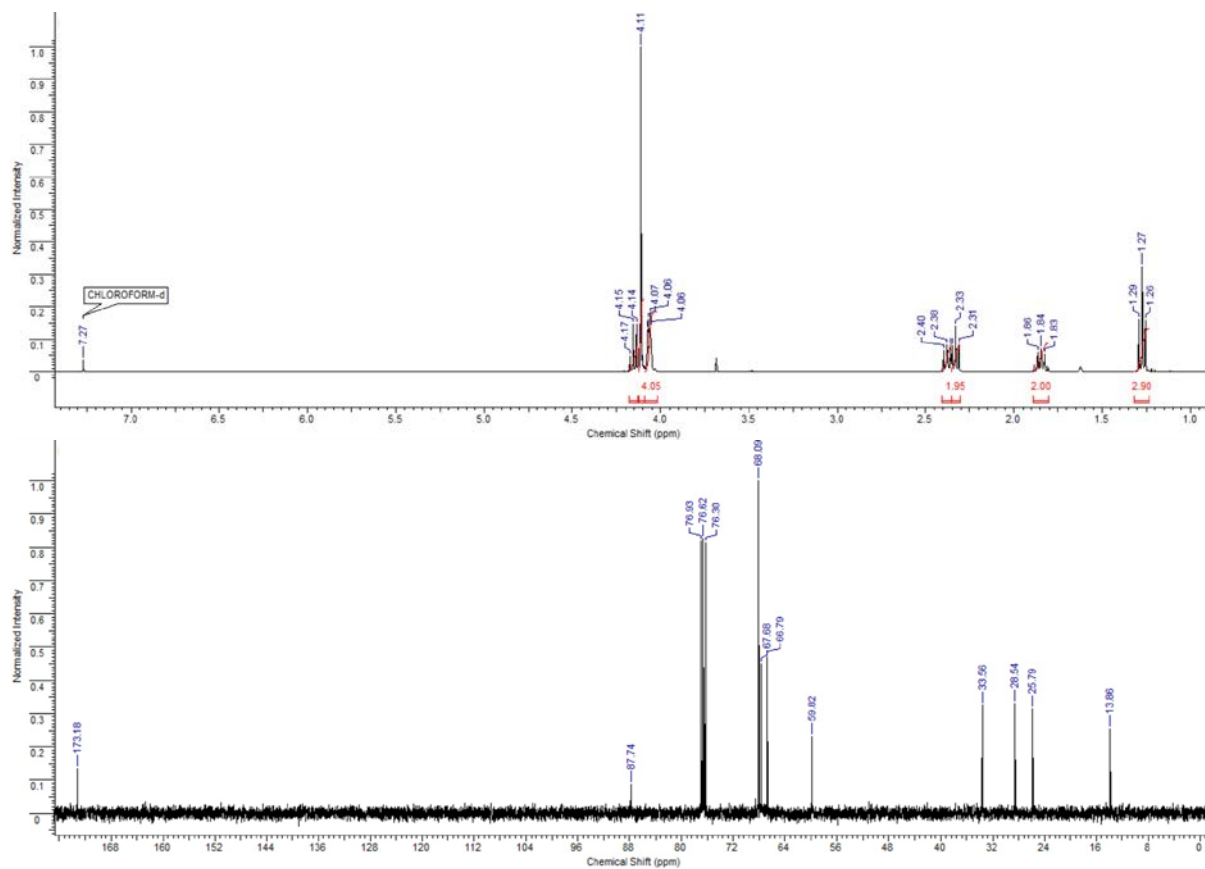
Fig. S51. ¹H, ¹³C NMR for compound **15**.

8. CV and RDE curves.
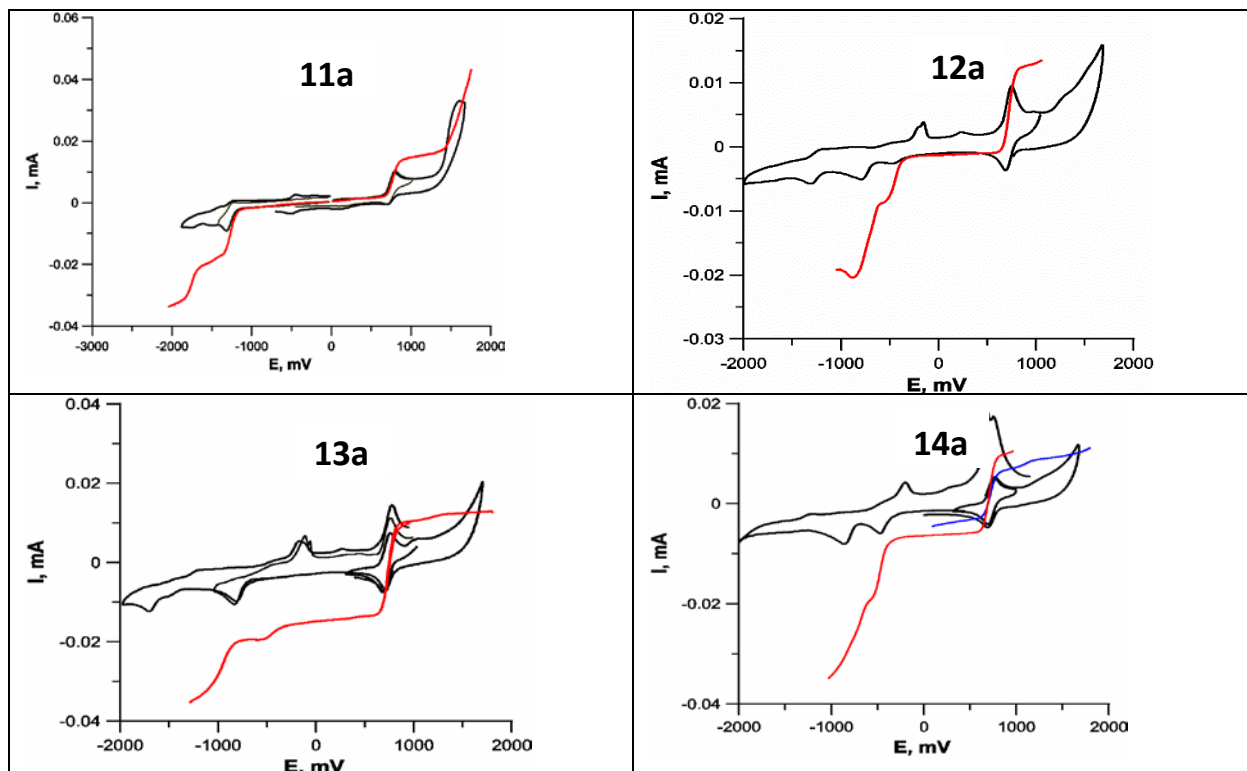
Fig. S52. CV and RDE graphs for compounds **11a – 14a**.
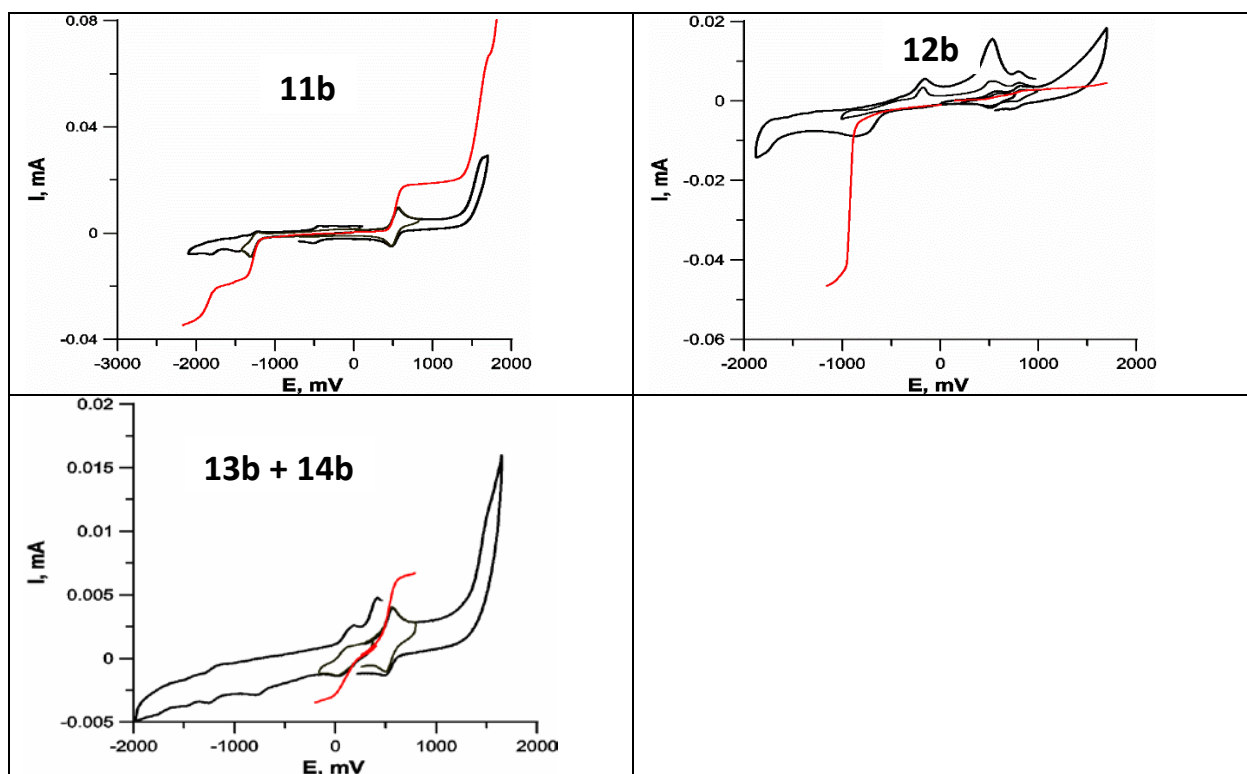
Fig. S53. CV and RDE graphs for compounds **11b – 14b**.
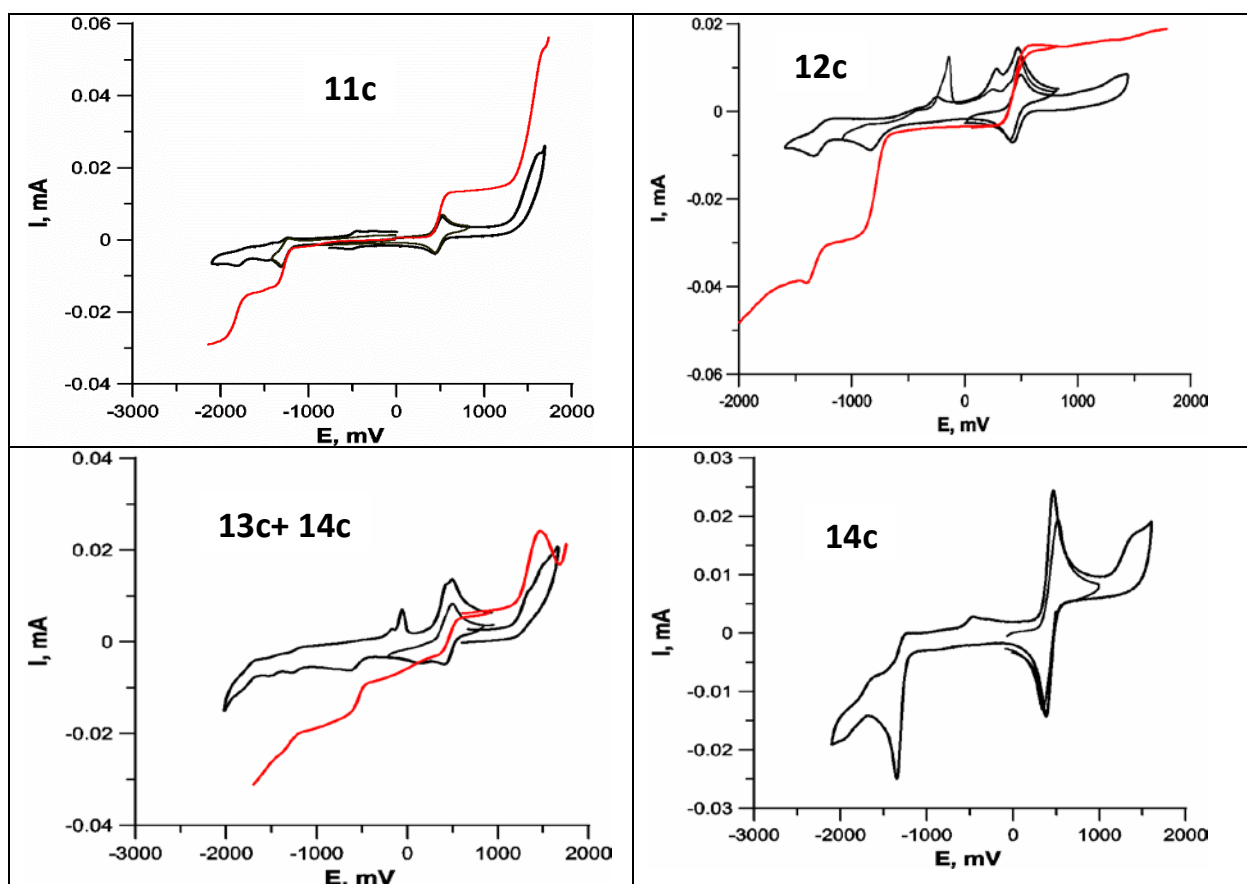
Fig. S54. CV and RDE graphs for compounds **11c – 14c**.
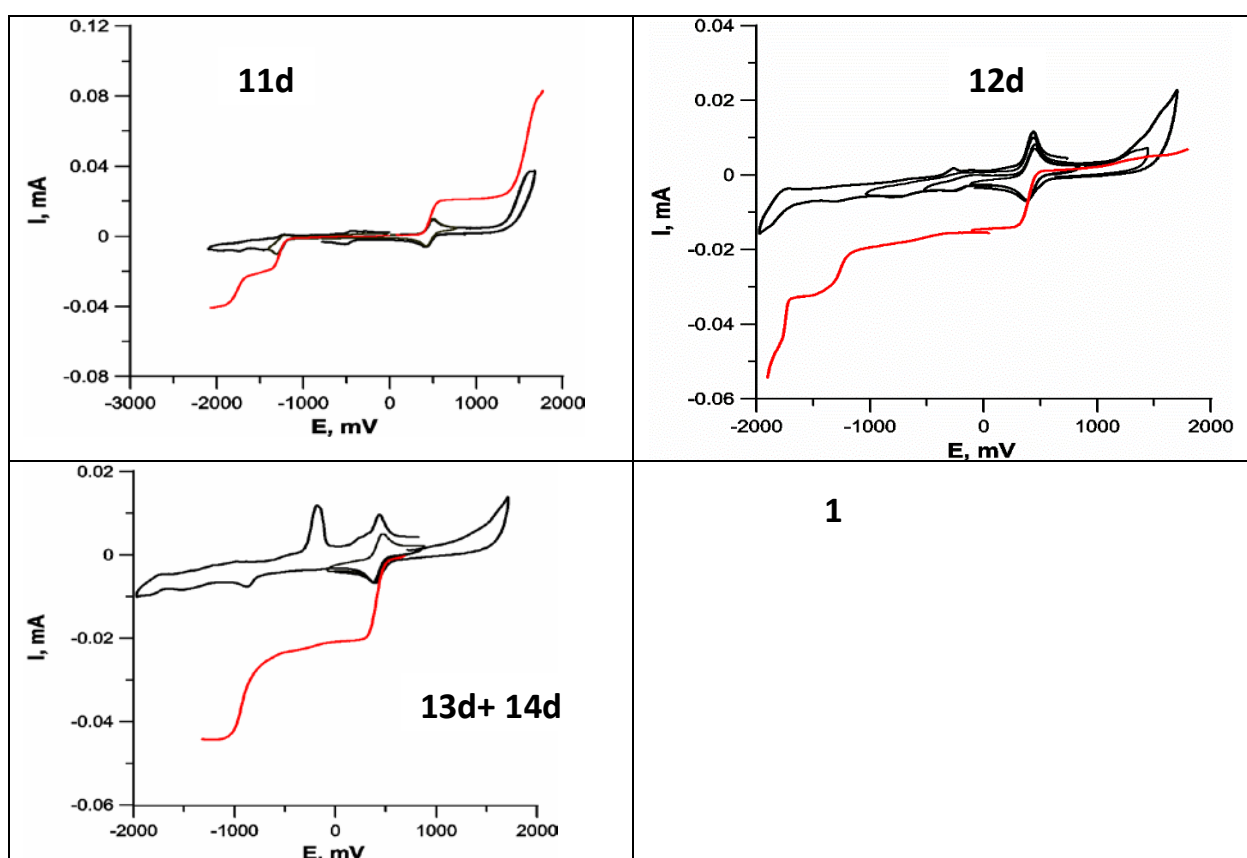
Fig. S55. CV and RDE graphs for compounds **11d – 14d**.
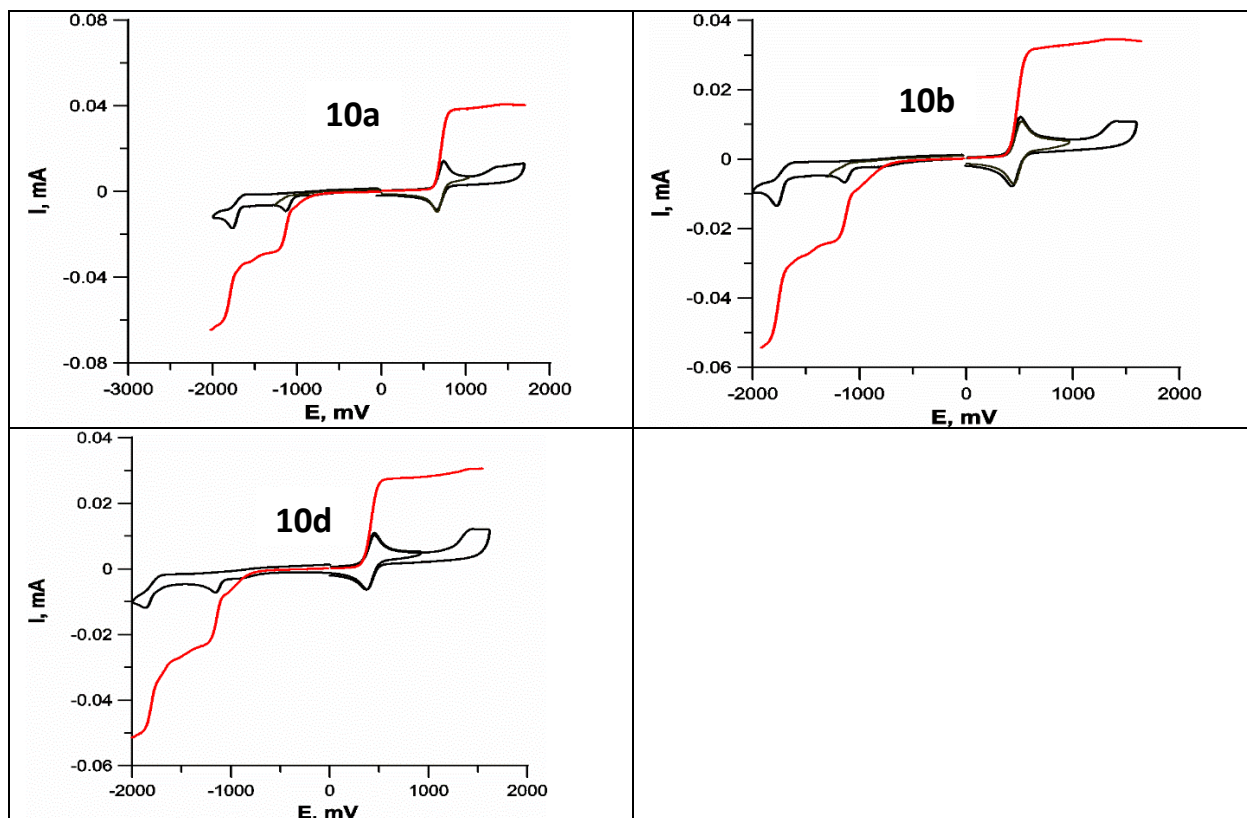
Fig. S56. CV and RDE graphs for compounds **10a, 10b, 10d**.

9. Study of the stability of coordination compounds and ligands in the cellular medium by electron spectroscopy.
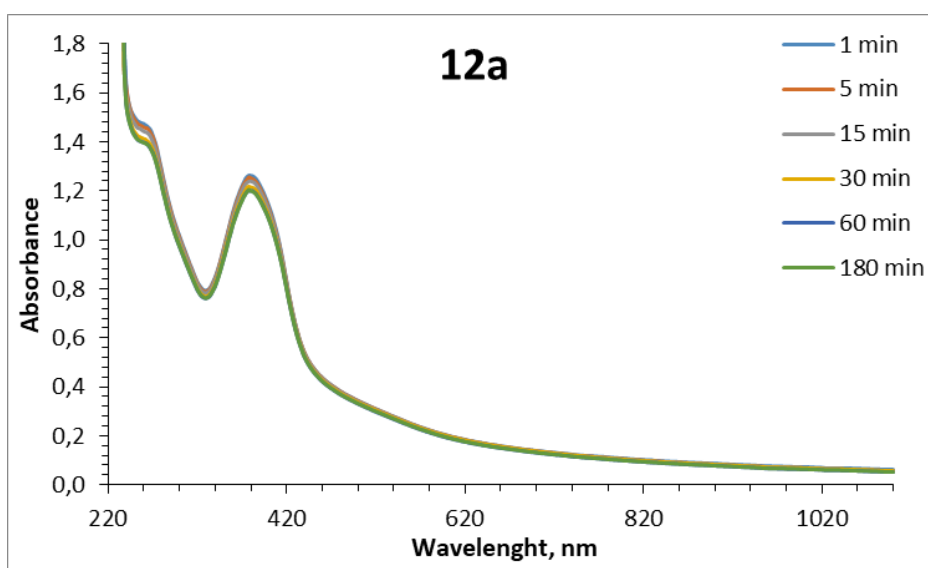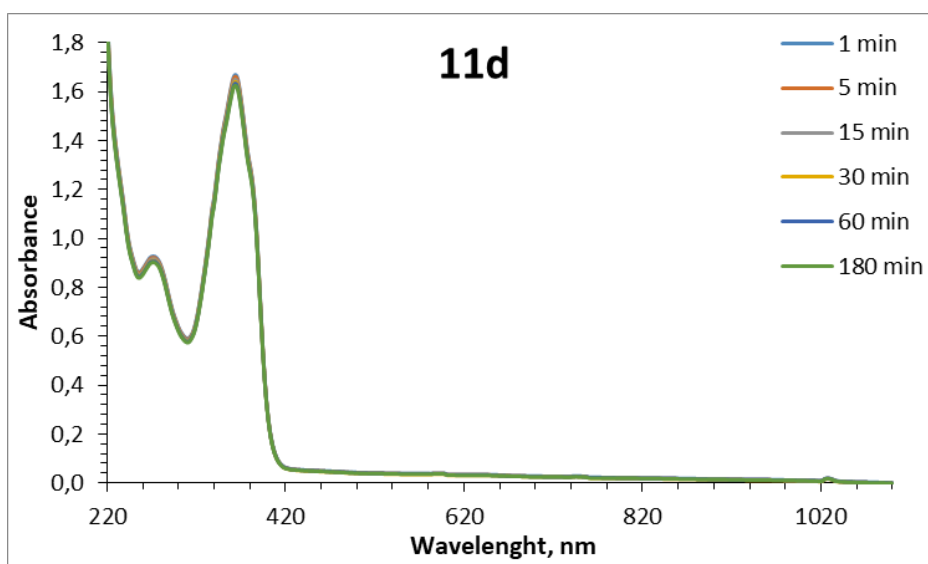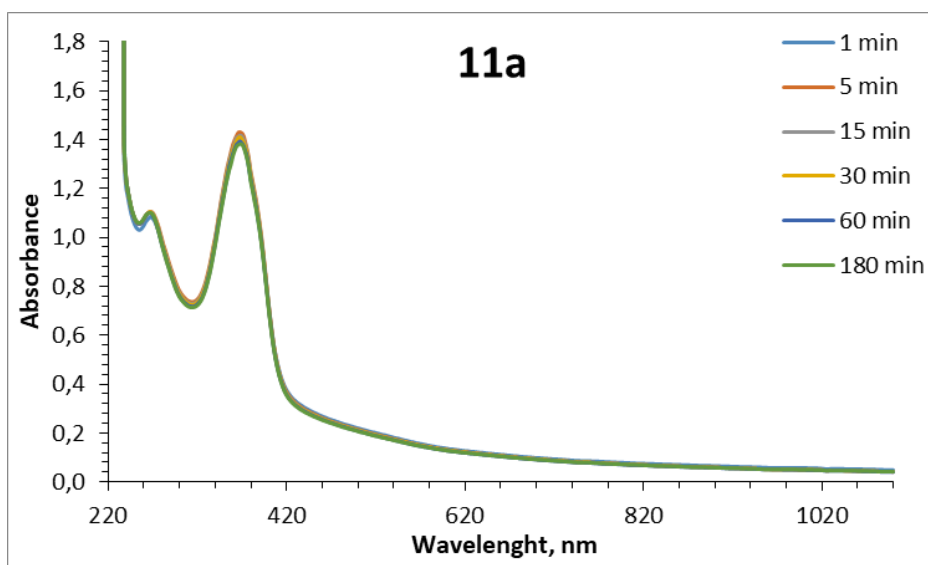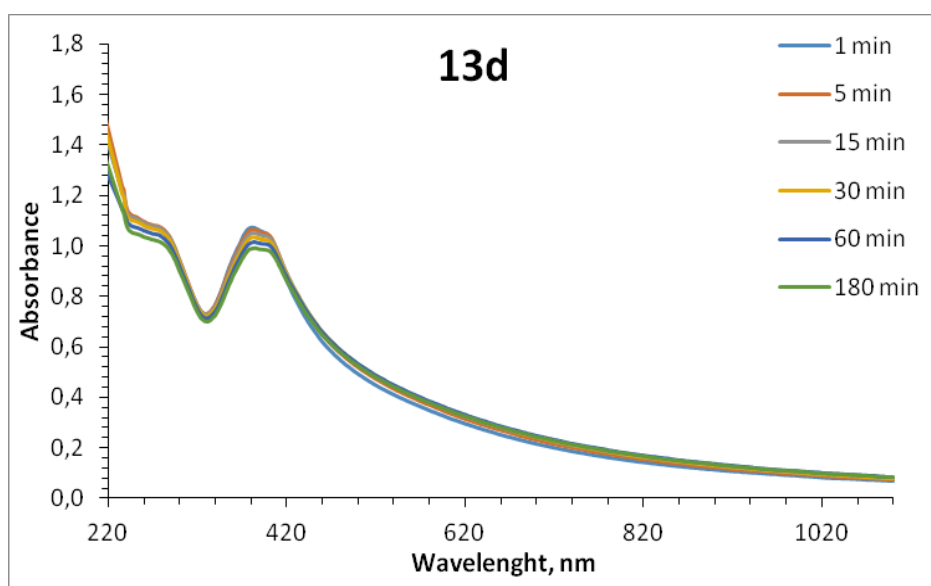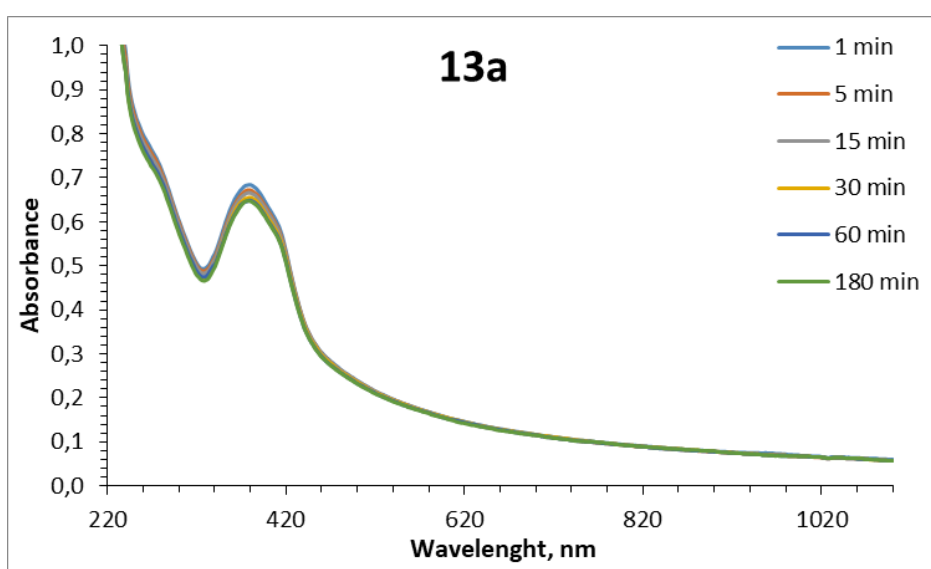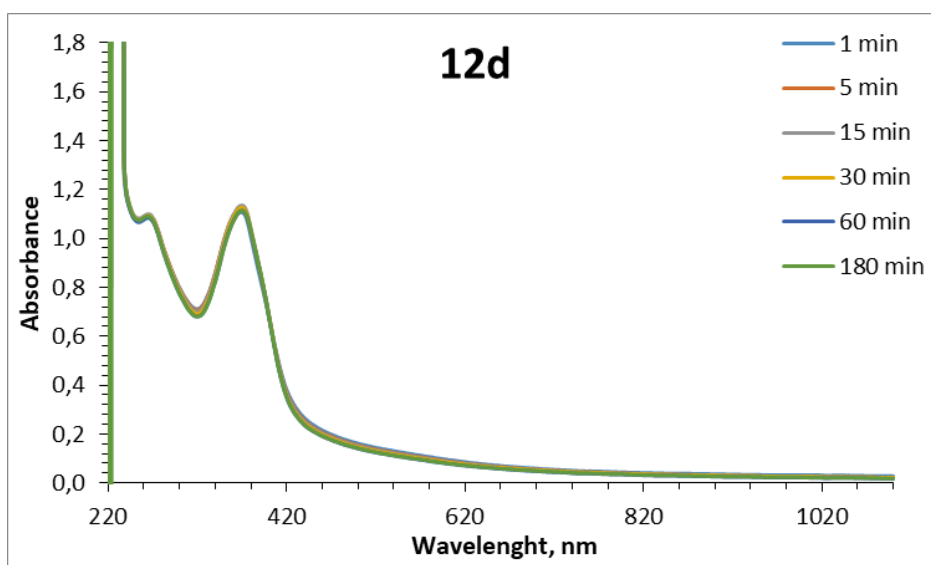
Fig. S57. UV-vis absorption spectra of the compounds **11a, 11d**, **12a, 12d**, **13a, 13d** in DMEM-F12 media (Gibco), C = 10^{-4} M.

10. Notes and references

1). Sheldrick, G. M. Acta Crystallogr. 2015, A71, 3-.8

2) Dolomanov, O.V., Bourhis, L.J., Gildea, R.J, Howard, J.A.K. & Puschmann, H. (2009), J. Appl. Cryst. 42, 339-341.

3). Brandenburg, K. DIAMOND, Release 2.1d; Crystal Impact GbR: Bonn, Germany, 2000.